

N89-12810

N89-12810

DEPARTMENT OF ELECTRICAL AND COMPUTER ENGINEERING

(NASA-CR-183001) FOCAL REGIONAL FIELDS OF
DISTORTED REFLECTORS Final Report (North
Carolina State Univ.) 72 p CSCI 20N

N89-12810

Unclas
G3/32 0174704



SCHOOL OF ENGINEERING

Final Report

NASA Grant NAG-1-738

**FOCAL REGION FIELDS OF
DISTORTED REFLECTORS**

N. E. Buris

J. F. Kauffman

**Department of Electrical and Computer Engineering
North Carolina State University
Raleigh, North Carolina 27695-7911**

July 1988

Focal Region Fields of Reflectors of Arbitrary Surface

Abstract

The problem of the focal region fields scattered by an arbitrary surface reflector under uniform plane wave illumination is solved. The Physical Optics (PO) approximation is used to calculate the current induced on the reflector. The surface of the reflector is described by a number of triangular domain-wise 5th degree bivariate polynomials. A 2-dimensional Gaussian quadrature is employed to numerically evaluate the integral expressions of the scattered fields. No Fresnel or Fraunhofer zone approximations are made. The relation of the focal fields problem to surface compensation techniques and other applications are mentioned. Several examples of distorted parabolic reflectors are presented. The computer code developed is included, together with instructions on its usage.

Introduction

Far field electromagnetic scattering from conducting surfaces of arbitrary shape has been studied by several researchers [1–6]. To our knowledge, however, little or no attention has been given to the near field scattering from arbitrary surfaces. The analysis of this problem may be useful to the efforts of compensation of reflector surface distortions. To illustrate this, let us consider the following situation. A plane wave, \bar{E}^i , is incident on an arbitrary reflector; the scattered fields, \bar{E}^s , in a region, Ω , in the neighborhood of the reflector are calculated by the method outlined in the present paper. Using the reciprocity theorem yields, if in Ω the fields \bar{E}^s are considered to be incident on the reflector, then the fields scattered by it will be \bar{E}^i . For antenna performance considerations \bar{E}^i is required to meet certain specifications. These specifications can be easily employed in the context of the method presented here and yield the \bar{E}^s fields in Ω . If Ω is chosen to be the region occupied by the feed, then \bar{E}^s is related to the excitation. Thus a scheme can be developed to provide the necessary excitation that renders desired far fields, \bar{E}^i , from a reflector antenna of arbitrary shape. In addition, focal field analysis may be applied to the problem of scattering by objects in the neighborhood of the feed and/or on the feed itself.

In the present paper, we develop a straightforward method to solve for the scattered fields (with emphasis in the near field zone) when a plane wave is incident on a reflector with arbitrary surface. The currents induced on the reflector are calculated by the Physical Optics (PO) approximation ($\bar{K} = 2\hat{n} \times \bar{H}^i$). Subsequently, these currents are used as sources of the scattered fields and explicit integral expressions of the latter in terms of \bar{K} are shown. These integrals expressions involve no approximation due to the position of the observation points with respect to the sources and, therefore, are valid for all zones

(near, Fresnel and Fraunhofer). Since we deal with rapidly oscillating integrands, accurate integration techniques are required and employed in the present work.

The novelty of our method consists of:

1. Triangular discretization of the reflector aperture by a max-min criterion based algorithm.
2. Reflector surface representation via interpolation of several fifth degree bivariate polynomials.
3. Development of a systematic, 2-dimensional, Gaussian quadrature calculation of the integrals involved in the scattered field expressions.

In this report, we examine the effects of various surface distortions on the focal region fields of parabolic reflectors. The performance of distorted reflectors with frequency is also discussed.

Theory

Let us consider a plane electromagnetic wave incident on an arbitrarily shaped and perfectly conducting surface, Σ , as in Figure 1. Let us also consider a Cartesian coordinate system $Oxyz$ such that the magnetic field of the incident wave is along the y axis and the wave vector is along the negative z axis. The surface of the reflector in this coordinate system is described by the function

$$z = g(x, y). \quad (1)$$

The fields of the incident wave are given by

$$\vec{H} = \hat{y} H_0 e^{j\beta z} \quad (2)$$

and

$$\overline{E} = -\hat{x}\eta H_0 e^{j\beta z} \quad (3)$$

where

$$\eta = \sqrt{\frac{\mu}{\epsilon}} \quad (4)$$

and β is the wavenumber. \hat{x}, \hat{y} and \hat{z} are the unit vectors along the axis of the $Oxyz$ coordinate system and η is the intrinsic impedance of the medium. According to the physical optics (PO) approximation, a surface current density \overline{K} is induced on the reflector.

This current density is the source of the scattered fields and is equal to

$$\overline{K}(\vec{r}) = 2\hat{n}(\vec{r}) \times \overline{H}(\vec{r}) \quad ; \quad \vec{r} \in \Sigma \quad (5)$$

where $\hat{n}(\vec{r})$ is the unit vector normal to the surface of the reflector. Using (1) we can obtain the expression

$$\hat{n}(\vec{r}) = \frac{\hat{z} - \nabla g(x, y)}{|\hat{z} - \nabla g(x, y)|} \quad (6)$$

Elaborating on Equation (6) and using Equation (2) and (5), the surface current density $\overline{K}(\vec{r})$ is derived to be

$$\overline{K}(\vec{r}) = 2H_0 \frac{-\hat{x} - \hat{z} \frac{\partial g}{\partial x}}{\sqrt{1 + \left(\frac{\partial g}{\partial x}\right)^2 + \left(\frac{\partial g}{\partial y}\right)^2}} e^{j\beta z} \quad (7)$$

The vector potential due to this current is

$$\overline{A}(\vec{r}) = \frac{1}{4\pi} \int_{\Sigma} \overline{K}(\vec{r}') \frac{e^{-j\beta|\vec{r}-\vec{r}'|}}{|\vec{r}-\vec{r}'|} d^2 r' \quad (8)$$

The magnetic and electric scattered fields are related to $\overline{A}(\vec{r})$ by

$$\overline{H}(\vec{r}) = \nabla \times \overline{A}(\vec{r}) \quad (9)$$

and

$$\bar{E}(\bar{r}) = \frac{1}{j\omega\epsilon} \nabla \times \nabla \times \bar{A}(\bar{r}). \quad (10)$$

Expanding Equation (10) we obtain the following integral expression of the electric field in terms of the current density.

$$\begin{aligned} \bar{E}(\bar{r}) = & \frac{1}{4\pi j\omega\epsilon} \int_{\Sigma} \frac{e^{-j\beta R}}{R} \left\{ \left[\bar{K}(\bar{r}') \cdot (\bar{r} - \bar{r}') \right] \frac{3 + 3j\beta R - \beta^2 R^2}{R^4} (\bar{r} - \bar{r}') \right. \\ & \left. - \frac{1 - \beta^2 R^2 + j\beta R}{R^2} \bar{K}(\bar{r}') \right\} d^2 r'. \end{aligned} \quad (11)$$

where ϵ is the dielectric permittivity of the environment and $\bar{R} = \bar{r} - \bar{r}'$. Equation (11) is in agreement with an alternative expression given by Silver [7]. The integration is carried over the illuminated portion of the reflector and $d^2 r'$ is the area element on Σ . If σ is the projection of Σ on the $x-y$ plane, the integral of Equation (11) can be performed on σ due to the relation dictated by Equation (1). Differential geometry considerations [2,8] yield the following relation between the area elements on Σ and σ , $d^2 r'$ and $dx'dy'$ respectively.

$$d^2 r' = \sqrt{1 + \left(\frac{\partial g(x', y')}{\partial x'} \right)^2 + \left(\frac{\partial g(x', y')}{\partial y'} \right)^2} dx'dy'. \quad (12)$$

Combining Equation (7) and (12) we obtain

$$\bar{E}(\bar{r}') d^2 r' = 2H_0 e^{j\beta z'} \left[-\hat{x} - \hat{z} \frac{\partial g(x', y')}{\partial x'} \right]. \quad (13)$$

Substituting Equation (13) into Equation (11) we get

$$\begin{aligned} \bar{E}(\bar{r}) = & \frac{2H_0}{4\pi j\omega\epsilon} \int_{\sigma} \frac{e^{-j\beta(R-z')}}{R} \left\{ \left[-(x-x') - (z-z') \frac{\partial g}{\partial x'} \right] \frac{3 + 3j\beta R - \beta^2 R^2}{R^4} (\bar{r} - \bar{r}') \right. \\ & \left. + \frac{1 - \beta^2 R^2 + j\beta R}{R^2} \left(\hat{x} + \hat{z} \frac{\partial g}{\partial x'} \right) \right\} dx'dy'. \end{aligned} \quad (14)$$

Normalized to the magnitude of the electric field of the incident wave and expressed in component form, Equation (14) yields

$$E_{sx}(\bar{r}) = \frac{1}{2\pi j\beta} \int_{\sigma} \frac{e^{-j\beta(R-z')}}{R} \left\{ \left[x - x' + (z - z') \frac{\partial g}{\partial x'} \right] \frac{\beta^2 R^2 - 3 - 3j\beta R}{R^4} (x - x') + \frac{1 - \beta^2 R^2 + j\beta R}{R^2} \right\} dx' dy' \quad (15)$$

$$E_{sy}(\bar{r}) = \frac{1}{2\pi j\beta} \int_{\sigma} \frac{e^{-j\beta(R-z')}}{R} \left\{ \left[(x - x') + (z - z') \frac{\partial g}{\partial x'} \right] \frac{\beta^2 R^2 - 3 - 3j\beta R}{R^4} (y - y') \right\} dx' dy' \quad (16)$$

$$E_{sz}(\bar{r}) = \frac{1}{2\pi j\beta} \int_{\sigma} \frac{e^{-j\beta(R-z')}}{R} \left\{ \left[x - x' + (z - z') \frac{\partial g}{\partial x'} \right] \frac{\beta^2 R^2 - 3 - 3j\beta R}{R^4} (z - z') + 1 - \beta^2 R^2 + \frac{j\beta R}{R^2} \frac{\partial g}{\partial x'} \right\} dx' dy' \quad (17)$$

Calculation of Integrals

The expressions of the scattered electric field in Equation (14) has been obtained by making only one approximation, namely the *PO* approximation (cf. Equation (5)). Since we are primarily interested in the focal region fields, the usual and convenient far field approximations cannot be used here. Neither can the Fresnel region approximations since we would like to treat geometries for which the focal point is in the near zone. Since we want to analyze arbitrary surfaces, a good way to represent the reflector is by a number of "target points." In an experimental version of this problem, target points would be small dots of an appropriate material placed on the surface of the reflector. We assume that the coordinates of these points can be measured by some technique (photogrammetric measurements). The projection of these points on the $x - y$ plane provides a natural discretization of the domain of integration σ (see Figure 2). We employ a max min criterion algorithm [9,10] to define triangles with vertices which are the projections of the target

points on σ . Since the collection of all triangles constitutes a polygonal approximation to σ , the integrals over σ can be found by simply calculating the contribution from each triangular domain and subsequently adding them up. For an analytical representation of the surface of the reflector, the same program mentioned above is used to interpolate a fifth degree bivariate polynomial in each triangular domain. This polynomial representation is used to estimate the values of z' and $\frac{\partial g}{\partial x'}$ on the surface of the reflector. Needless to say, the larger the number of target points and, thus, triangles on σ , the better the representation of Σ . The integral of Equation (14) is not only vectorial but, it is complex as well. Therefore, numerically we need to perform six integrations in order to find the real and imaginary parts of all three components of the electric field at an arbitrary point $\vec{r} = \hat{x}x + \hat{y}y + \hat{z}z$. The functions to be integrated can be very oscillatory in nature due to the phase term $\exp(-j\beta(r - z'))$ and also due to the presence of the $\partial g/\partial x'$ term. As is well known [11,12] there are no satisfactory quadrature formulae to integrate functions on triangular domains. However, a series of mappings can be employed to transform a triangle into a square (see Figure 3). There, a simple extension of the one-dimensional Gaussian Quadrature is available. A brief outline of this method follows.

By means of a linear transformation, every triangle of the x - y plane can be mapped onto a specific triangle in another plane, u - v . Consider an arbitrary triangle in the $x - y$ plane with vertices (x_1, y_1) , (x_2, y_2) and (x_3, y_3) . This arbitrary triangle can be mapped onto a basic triangle in another coordinate system, $u - v$, by the transformation:

$$x = x_1 + au + bv \quad (18a)$$

$$y = y_1 + cu + dv \quad (18b)$$

where

$$a = x_2 - x_1 \quad (19)$$

$$b = x_3 - x_1 \quad (20)$$

$$c = y_2 - y_1 \quad (21)$$

and

$$d = y_3 - y_1 \quad (22)$$

The Jacobian of mapping (18) is

$$J \left(\frac{x, y}{u, v} \right) = \begin{vmatrix} a & b \\ c & d \end{vmatrix} = (ad - bc) = (x_2 - x_1)(y_3 - y_1) - (x_3 - x_1)(y_2 - y_1). \quad (23)$$

The inverse transformation is

$$u = [d(x - x_1) - b(y - y_1)] / (ad - bc) \quad (24a)$$

$$v = [-c(x - x_1) + a(y - y_1)] / (ad - bc). \quad (24b)$$

According to (18), the vertices $A = (x_1, y_1)$, $B = (x_2, y_2)$ and $C = (x_3, y_3)$ are mapped onto the points $[0, 0]$, $[1, 0]$ and $[0, 1]$, respectively, in the $u - v$ coordinate system. These points define what we call the basic triangle in the $u - v$ system. As mentioned above, there are no satisfactory quadrature formulae for integration on triangular domains for rapidly oscillatory integrands. The basic triangle in the $u - v$ system can be mapped onto a square domain by means of the transformation

$$u = \frac{1 + r}{2} \quad (25a)$$

$$v = \left(\frac{1 - r}{4} \right) (1 + s). \quad (25b)$$

The Jacobian of mapping (25) is

$$J \left(\frac{u, v}{r, s} \right) = \begin{vmatrix} 1/2 & 0 \\ -\frac{1+s}{4} & \frac{1-r}{4} \end{vmatrix} = \frac{1 - r}{8}. \quad (26)$$

According to (25), the sides $v = 0$ and $v = 1 - u$ of the basic triangle are mapped onto the lines $s = -1$ and $s = +1$ respectively, in the $r - s$ coordinate system. Similarly, the side $u = 0$ is mapped onto the line $r = -1$ and, the point B is mapped onto the line $r = 1$. In Figure 2, we show the series of mappings described above.

An integral over D_{xy} can be numerically calculated using a Gaussian quadrature formula on the square domain D_{rs} provided we represent the integrand appropriately. Thus, if $f(x, y)$ is a function defined over the triangular domain D_{xy} and I is the integral

$$I = \int_{D_{xy}} \int f(x, y) dx dy, \quad (27)$$

we know that

$$I = \int_0^1 \int_{v=0}^{1-u} f(x(u, v), y(u, v)) J \left(\frac{x, y}{u, v} \right) du dv \quad (28)$$

and also

$$I = \int_{-1}^1 \int_{-1}^1 f \left(x \left(u(r, s) \right), y \left(u(r, s), v(r, s) \right) \right) J \left(\frac{x, y}{u, v} \right) J \left(\frac{u, v}{r, s} \right) dr ds. \quad (29)$$

For our purposes, Equation (29) essentially looks like

$$I = \int_{-1}^1 \int_{-1}^1 T(r, s) dr ds. \quad (30)$$

where

$$T(r, s) = f(x, y) J \left(\frac{x, y}{u, v} \right) J \left(\frac{u, v}{r, s} \right) \quad (31)$$

An obvious 2-dimensional extension of the well-established 1-dimensional quadrature formulae is used here. That is

$$I \simeq \int_{-1}^1 \sum_{j=1}^N W_j T(r, s_j) dr,$$

and, finally

$$I \simeq \sum_{k=1}^N \sum_{j=1}^N W_k W_j T(r_k, s_j). \quad (32)$$

In our analysis r_k and s_j ($k, j = 1, 2, \dots, N$) are the roots of the N^{th} order Legendre polynomial, P_N , and W_k ($k = 1, 2, \dots, N$) are the appropriate weights for Gaussian quadrature, given by

$$W_k = \frac{2}{(1 - r_k^2) P'_N(r_k^2)}. \quad (33)$$

From (32) it is clear that the values of T are required at the points (r_k, s_j) of the $r - s$ coordinate system. Using the transformations (25) and (18), the corresponding points (x_{kj}, y_{kj}) of the $x - y$ coordinate system can be found. It is clear that

$$f(x_{kj}, y_{kj}) = F(r_k, s_j). \quad (34)$$

There are N^2 points in each triangle. The value of N required to accurately calculate the integrals depends on the frequency and the surface of the reflector. It is found that if the reflector has extensive distortions, a large N is required.

One subtle point needs to be mentioned here. Since the square domain D_{rs} and the basic triangle domain D_{uv} are fixed and kept the same for all $x - y$ triangles, the limits of integration in (28) and (29) are desired to stay fixed. As a consequence, A, B, and C must be in a counter-clockwise sense. It is important that the vertices of all the D_{xy} triangles be arranged in the same rotational sense. If instead of the counter-clockwise sense presented here, a clockwise sense were chosen, then the Jacobian $J \left(\frac{x, y}{u, v} \right)$ would need a sign reversal to ensure the correct result.

To recapitulate, the projection, σ , of the reflector on the $x - y$ plane is divided in a number of triangles. The integrals of Equations (15)–(17) are decomposed into summations of integrals over the aforementioned triangles. For each triangle, the points (x_{kj}, y_{kj}) are

found by applying (25) and (18). Then, the quadrature formula (32) is used to evaluate the contribution of each triangle to the total integral. Finally, all these contributions are added together to yield approximate values for E_{sx} , E_{sy} and E_{sz} .

Oblique Incidence

The generic geometry presented in the second section can be used to solve the problem of the scattered fields of a given reflector under oblique incidence. To demonstrate this assertion, consider a coordinate system $O\tilde{x}\tilde{y}\tilde{z}$, attached to the reflector. The relative orientation of the reflector system, $O\tilde{x}\tilde{y}\tilde{z}$, and the incident wave system, $Oxyz$, is described by the Euler angles θ , ϕ and ψ as shown in Figure 4.

To solve for the scattered fields under these circumstances, we make use of the fact that $g(x, y)$ in Equation (1) is arbitrary. If the reflector in its own coordinate system is described by $\tilde{z} = g(\tilde{x}, \tilde{y})$, then we can express this reflector in $Oxyz$ and then use the analysis of Section 2. To do this we perform three rotations. First a positive rotation about $O\tilde{z}$ by ϕ . This rotation moves $O\tilde{y}$ to a new position $O\tilde{y}'$. The second rotation is about $O\tilde{y}'$ by $+\theta$. This rotation aligns the optical axis of the reflector with Oz . Finally, a third rotation about Oz by an amount ψ is required to align $O\tilde{y}'$ with Oy and thus take care of the polarization.

The sequence of rotations is shown in Figure 5. To demonstrate the use of these rotations, consider the following special cases.

1. Incident wave \vec{E}^i on the $O\tilde{x}\tilde{y}$ plane and \vec{H}^i field perpendicular to the $O\tilde{x}\tilde{z}$ plane (see Figure 6). Thus, $\phi = 0$ and $\psi = 0$.

2. Propagation along the negative $0 \tilde{z}$ axis (see Figure 7). Thus, $\theta = 0$, $\phi = 0$, and $\psi = \psi$. Please note that you need to rotate the $0 \tilde{x}\tilde{y}\tilde{z}$ system to make it align with the $Oxyz$ system. Furthermore, the values of θ, ϕ , and ψ have to be positive for counterclockwise rotations and negative for clockwise ones.

Numerical Examples

In an experimental application of the analysis presented above, the coordinates of the target points would be measured and provided as data to the developed computer code. Since this report does not involve experimental studies, an analytical method is needed to generate the coordinates of the target points. First we distribute the projections of the target points onto the $0\tilde{x}\tilde{y}$ plane. We do this by locating all of these points on circles of successively increasing radius up to a given value. The number of points on each circle also increases as we move outwards. This scheme of discretization is suitable for circular aperture reflectors and is shown in Figure 8. In this discretization example, we have used four circles with radius and points as follows.

Circle #	Radius	Points on Circle
0	0	1
1	1	$np = 3$
2	2	$2np = 6$
3	3	$2(2np)=12$

This scheme provides us with the \tilde{x} and \tilde{y} coordinates of the target points. To complete the description of the surface of the reflector, a function is needed to generate the \tilde{z} coordinates of the targets. For all the examples presented in this section, the target points lay on a

surface generated by the function

$$\tilde{z} = \frac{\tilde{x}^2 + \tilde{y}^2}{4F} + A_1 e^{A_2[(\tilde{x}-A_3)^2 + (\tilde{y}-A_4)^2]} \quad ; \quad \tilde{x}^2 + \tilde{y}^2 \leq \frac{D^2}{4} . \quad (35)$$

Clearly, Equation (35) represents an ideal paraboloid of focal length, F , that is perturbed by a Gaussian “bump” of height, A_1 , steepness, A_2 , located at the point $(\tilde{x}, \tilde{y}) = (A_3, A_4)$. For $A_1 = 0$ Equation (35) represents an ideal parabolic reflector of diameter, D . We are primarily interested in the fields of the focal region. The observation points in this section will be assumed to be distributed on a line segment of electrical length $\beta\ell$ that has its origin at the point 0_b on the z -axis and is parallel the the $0\tilde{x}\tilde{y}$ plane (see Figure 9).

In Figure 10, the magnitude of the electric field components is shown for an ideal paraboloid with diameter, $D = 2\text{m}$, focal length, $F = 1.19\text{m}$, at frequency, $f = 500\text{ MHz}$. The observation points are defined by $\phi_{ob} = 0$ and $\beta\ell = 20$, i.e., they lay on the $0_b\tilde{x}$ axis. In this example $\phi = \theta = \psi = 0^\circ$, i.e., the coordinate systems $0xyz$ and $0\tilde{x}\tilde{y}\tilde{z}$ are identical. That is the incident field is propagating along the negative $0\tilde{z}$ axis and has its $\overline{H}(\overline{E})$ field along the $0\tilde{y}(0\tilde{x})$ axis. It is clear from Figure 10 that the cross polar field, E_y , is very weak, negligible in comparison to E_x and E_z . In Figure 11, the magnitude of the electric field components of a perturbed version of the paraboloid of the previous example is shown. The characteristics of the perturbation are $A_1 = 0.1\text{m}$, $A_2 = -3$, and $A_3 = A_4 = 0.2\text{m}$. A comparison between Figure 10 and 11 reveals that the surface perturbation has quantitative effects on the focal region fields. First, the co-polar component has a maximum decreased by 10% from the corresponding value of the ideal surface case. Second, the cross-polar level is somewhat increased and third, the E_z component is no longer zero at the point 0_b .

In Figure 12, the magnitude of the normalized electric field components of the same distorted reflector used in Figure 11 is shown. The only difference between Figure 11 and 12 is the frequency. In Figure 11, the frequency is 5 GHz. The observation points are

again distributed on the $0_b \tilde{x}$ axis and $\beta\ell$ is the same as earlier ($\beta\ell = 20 \rightarrow \ell \approx 20$ cm). As is expected, because of the higher frequency, the bump on the surface of the reflector has more severe effects now than in Figure 11. To illustrate this, we compare the focal fields of the distorted reflector with the fields of the ideal reflector at $f = 5$ GHz. This comparison is depicted in Figures 13a–13f. From Figure 12, we see that the cross-polarized field component (E_y) is eight times smaller than the coplanar component or, down by 18 dB. We also see that, as in Figure 11, the axial field at the point 0_b is not zero when the surface has been distorted. Furthermore, we note that the phase of the cross-polar field component of the ideal surface parabolic reflector is not significant since the magnitude of the cross-polar field is zero (Figure 13b). Because of this fact, the phase of the cross-polar component of the ideal reflector is shown to exhibit a rather large numerical inaccuracy (Figure 13e). We may also point out that there is a significant increase (from 3.5 to 37) of the normalized coplanar component when we go from $f = 500$ MHz to $f = 5$ GHz (see Figures 10 and 13a). This is in accord to the well known limit of infinite focal fields at the Geometric Optics (GO) approximation.

Exactly the same number of target points has been used for all of the examples presented above. Furthermore, the coordinates of these points in the $0\tilde{x}\tilde{y}$ plane were also exactly the same. This enabled us to compare the results of the various test cases used. It is important to realize that, in general, the domain-wise 5th degree polynomial interpolation only approximates the surface of the reflector. As a consequence, if one uses two different sets of x - y coordinates of target points to represent a given reflector surface (for example given by Equation (35)), different scattered fields will be obtained under the same conditions of illumination. This problem, however, can be solved very easily by increasing the number of target points to achieve good polynomial representation of the

reflector surface. Numerical verification of this solution has been done, and we have found that the higher the frequency, the larger the number of target points required to represent the reflector in order to achieve convergence of the scattered fields.

At $f = 35$ GHz, and when the propagation is along the optical axis, the focal region fields of ideal parabolic receiving antennas obtained by the method of the present report have been found in complete agreement with the numerical results obtained by a different method (expansion in spherical wave functions) as in [13]. For arbitrary illumination and/or reflectors, however, we have not found studies by other researchers to cross-examine our numerical results.

In these cases, the scattered fields at a few observation points are calculated using various densities of points in the Gaussian quadrature (this is equivalent to varying N in Equation (32)) until convergence is achieved. For a given frequency, we have found that the smoother the surface of the reflector (the smaller A_1 in Equation (35)), the smaller N is required for convergence of the fields. To demonstrate this process, the ideal parabolic reflector used earlier ($D = 2\text{m}$, $F = 1.19\text{m}$) is subject to obliquely incident illumination ($\theta = 5^\circ, \phi = 0, \psi = 0$). In contrast to the previous examples, now the antenna ($0\tilde{x}\tilde{y}\tilde{z}$) and the ray ($0\tilde{x}\tilde{y}\tilde{z}$) coordinate systems are not identical. The normalized incident field, \overline{E}^i/E_0 in the two systems is

$$\frac{\overline{E}^i}{E_0} = -\hat{x}e^{j\beta z} = -\left(\hat{\tilde{x}}\cos 5^\circ - \hat{\tilde{z}}\sin 5^\circ\right)e^{j\beta(\tilde{x}\sin 5^\circ + \tilde{z}\cos 5^\circ)}. \quad (36)$$

The observation points are distributed on the negative \tilde{x} -axis, i.e., $\phi_{0b} = 180^\circ$ and $\beta\ell = 20 \rightarrow \ell \simeq 20$ cm. The geometry is shown in Figure 14. The magnitude of the normalized electric field components in the antenna coordinate system is plotted in Figures 15, 16, and 17 for various values of $N = ng$. From these figures, it is evident that convergence is

achieved very quickly. Note that the \tilde{y} -component is the smallest of all; about four orders of magnitude smaller than the \tilde{x} and \tilde{z} components. Convergence of the \tilde{y} -component is, however, still very rapid. In Figure 15, we observe that the scattered field has a maximum at a distance $\tilde{x}_0 = -11.2$ cm. If we interpret this in degrees from the optical axis, we find that the maximum of the scattered field occurs at an angle, θ_0 , where

$$\theta_0 = \tan \left| \frac{\tilde{x}_0}{F} \right| \simeq 5.38^\circ. \quad (37)$$

This was expected, since the angle of incidence, θ , is $\theta = 5^\circ$.

As an additional example, consider the previous case when the reflector is distorted by a bump located at the origin. The surface of the reflector is described by Equation (34) with parameters $D = 2\text{m}$, $F = 1.19\text{m}$, $A_1 = 0.1\text{m}$, $A_2 = -3$, $A_3 = 0$, and $A_4 = 0$. The frequency is again $f = 5$ GHz, and the incident illumination is described by Equation (36); i.e., $\theta = 5^\circ$, $\phi = 0$, $\psi = 0$. The magnitude of the normalized components of the scattered field on the negative \tilde{x} -axis ($\phi_{ob} = 180^\circ$, $\beta\ell = 20$) is shown in Figures 18, 19 and 20 for various $N = ng$. The convergence is achieved rapidly, especially for the major components of the field ($E_{\tilde{x}}$ and $E_{\tilde{z}}$). Comparing the undistorted (Figure 15, 16, and 17) with the distorted (Figure 18, 19, and 20) we observe that the largest field component, $E_{\tilde{x}}$, suffers a severe reduction (by a factor of 5) from its level at the absence of distortion. The $E_{\tilde{z}}$ component suffers a comparable reduction. Moreover, the level of the smallest field component, $\overline{E}_{\tilde{y}}$, is increased (by an order of magnitude) due to the distortion.

The parameter $A_1 = 0.1\text{m}$ used in the examples of distorted reflector examples is a rather extensive distortion, since it represents 10% of the radius of the reflector. In practical applications less severe distortions are expected. The higher the frequency, f , the larger the angle of incidence, θ , the larger N is required to achieve convergence.

Conclusions

A straightforward method to calculate the magnitude and phase of all three components of the focal region field scattered by an arbitrary reflector under plane wave illumination is presented. Discretization of the surface of the reflector and subsequent interpolation by fifth degree bivariate polynomials is made. The current induced on the reflector is evaluated by the PO approximation. The scattered field is given in an integral expression that involves no Fresnel or Fraunhofer zone approximations. A novel approach to the problem of numerical integration of the integrals is discussed. This method is based on a 2-dimensional Gaussian quadrature and provides a high degree of flexibility since the density of the sample points can be varied interactively as to adapt to the accuracy needs of the specific application. Several examples of distorted and undistorted parabolic reflectors are presented. The behavior of the scattered field with frequency and angle of incidence is discussed.

References

- [1] Chan, K. K. and Raab, A. R., "Surface Current Analysis of Distorted Reflector Antennas," IEE Proc., Vol. 128, No. 4, August 1981.
- [2] Rahmat-Samii, Y. and Galindo-Israel, V., "Shaped Reflector Antenna Analysis Using the Jacobi-Bessel Series," IEEE Trans. Antennas and Propagation, Vol. AP-28, No. 4, July 1980.
- [3] Ruze, J., "The Effect of Aperture Errors on the Antenna Radiation Pattern," Suppl. al Nuovo Cimento, Vol. 9, No. 3, pp 364-380, 1952.
- [4] Ruze, J., "Antenna Tolerance Theory — A Review," Proc. IEEE, Vol. 54, No. 4, April 1966.
- [5] Rahmat-Samii, Y. "A Generalized Reflector/Array Surface Compensation Algorithm for Gain and Sidelobe Control," IEEE Antennas and Propagation Symposium Proceedings, Blacksburg, VA, 1987, Vol. II, pp. 760-763.
- [6] Lee, T. H., Ruddock, R. C., and Bailey, M. C., "Pattern Calculations of Reflector Antennas with Surface Errors," IEEE Antennas and Propagation Symposium Proceedings, Blacksburg, VA, 1987, Vol. II, pp. 764-767.
- [7] Silver, S., ed., *Microwave Antenna Theory and Design*, §3.9-3.11, Peter Peregrinus Ltd., London, UK, 1984.
- [8] Guggenheimer, H. W., *Differential Geometry*, Dover Publications, Inc., New York, 1977.

- [9] Akima, H., "A Method of Bivariate Interpolation and Smooth Surface Fitting for Irregularly Distributed Data Points," ACM Trans. Math Software, Vol. 4, No. 2, June 1978, pp. 148-159.
- [10] Akima, H., "A Method of Bivariate Interpolation and Smooth Surface Fitting for Values Given at Irregularly Distributed Points," OT Rep. 75-70, U. S. Govt. Printing Office, Washington, D.C., August 1975.
- [11] Bramble, J. H. and Zlamal, M., "Triangular Elements in the Finite Element Method," Math. Comp., 24 (1980).
- [12] Davis, P. J., and Rabinowitz, P., *Methods of Numerical Integration*, Academic Press, New York, 1975.
- [13] Kennaugh, E. M. and Ott, R. H., "Fields in the Focal Region of a Parabolic Receiving Antenna," Report 1223-16, The Antenna Laboratory, Ohio State University, 31 August 1963.

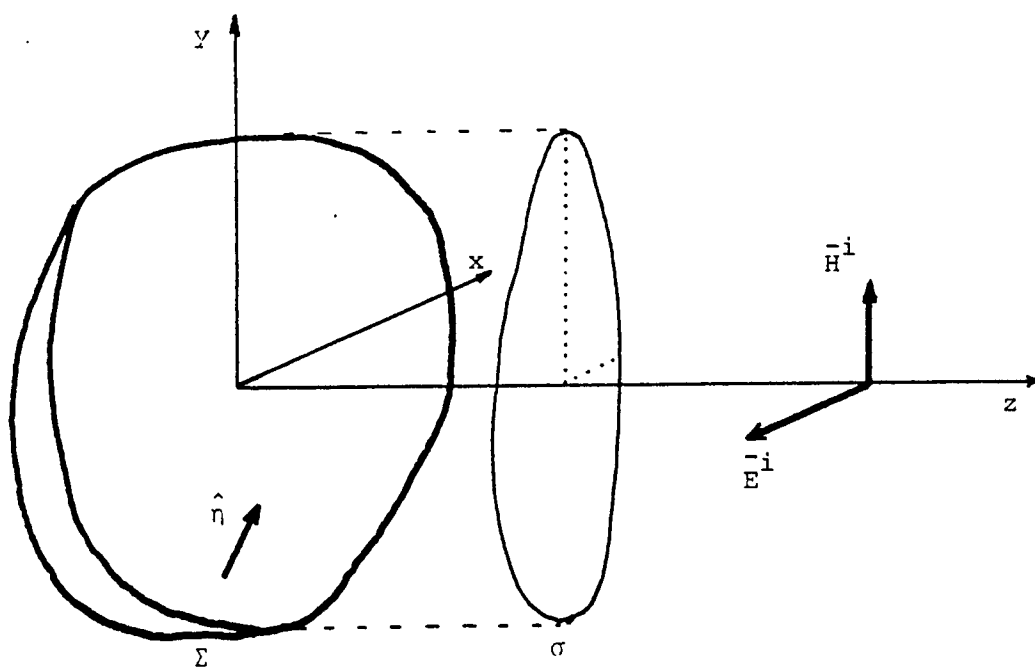


Figure 1. Arbitrary Reflector Geometry

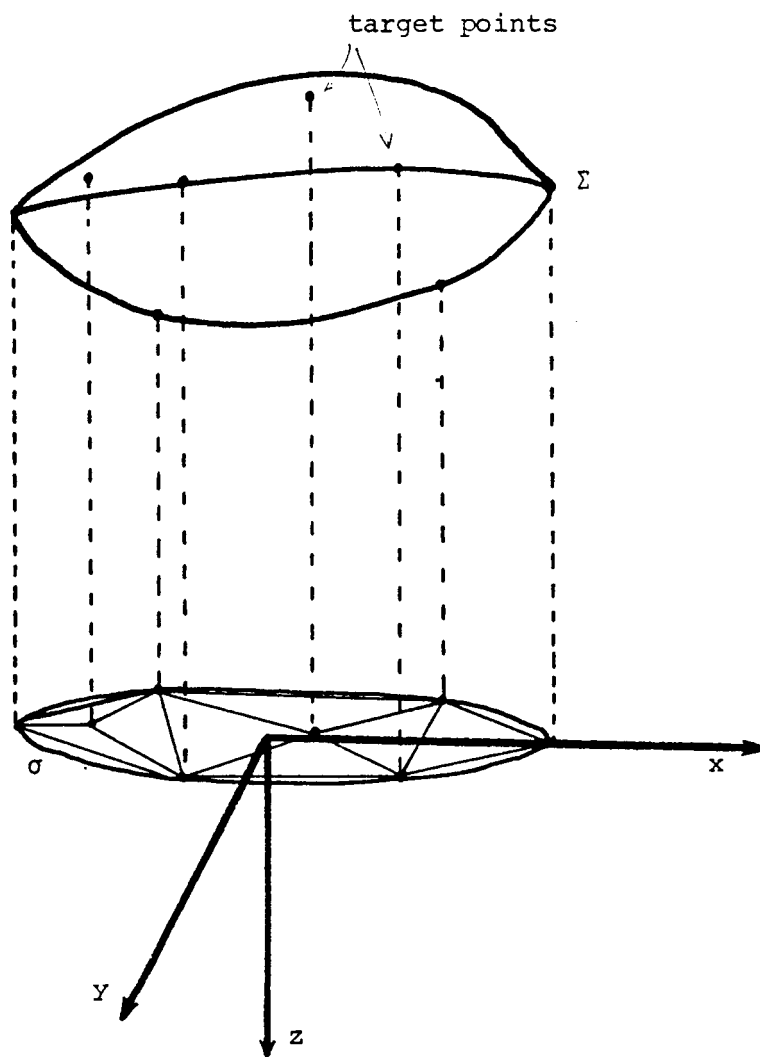


Figure 2. Reflector Discretization

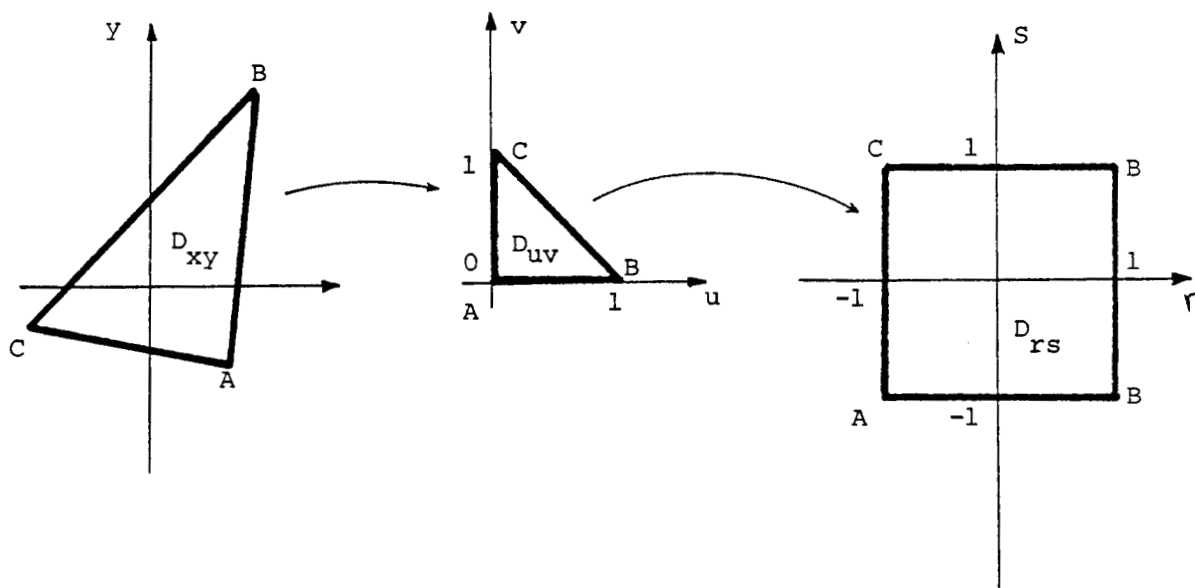


Figure 3. Successive mapping of an arbitrary triangle onto a basic one and, then, a square

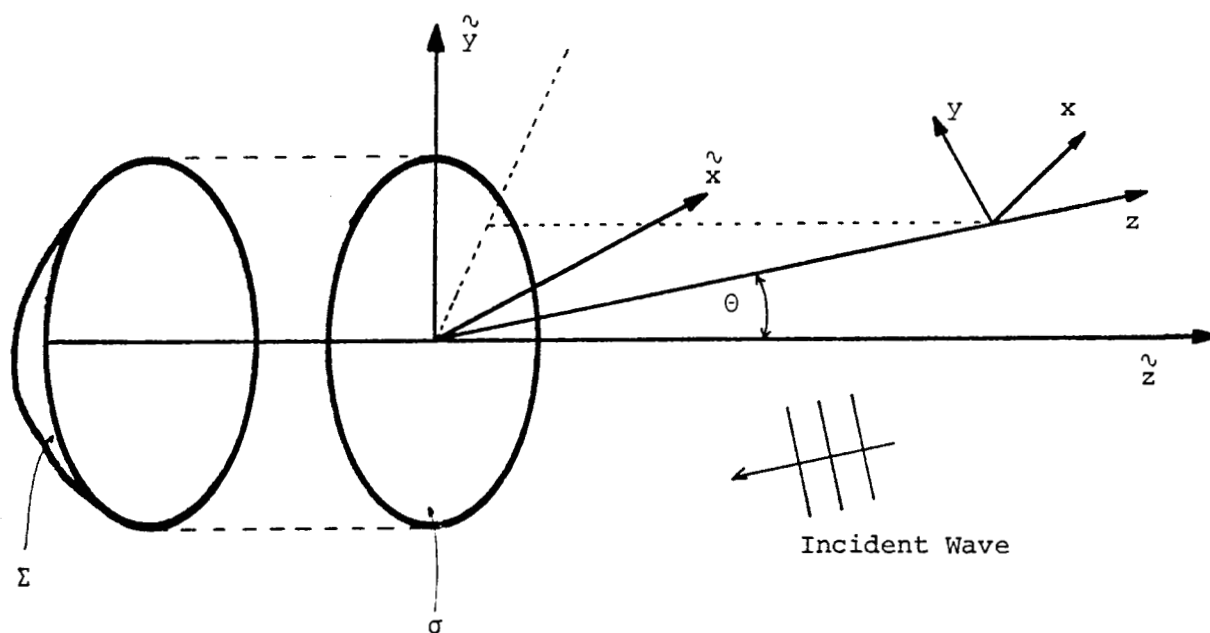


Figure 4. Relative orientation of antenna and ray coordinate systems.

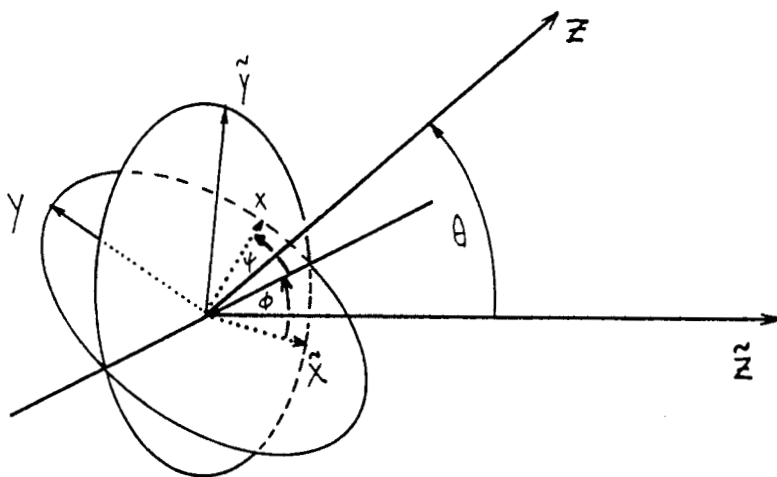


Figure 5. Euler's angles θ , ϕ and ψ define the relative orientation between the antenna and the ray coordinate system.

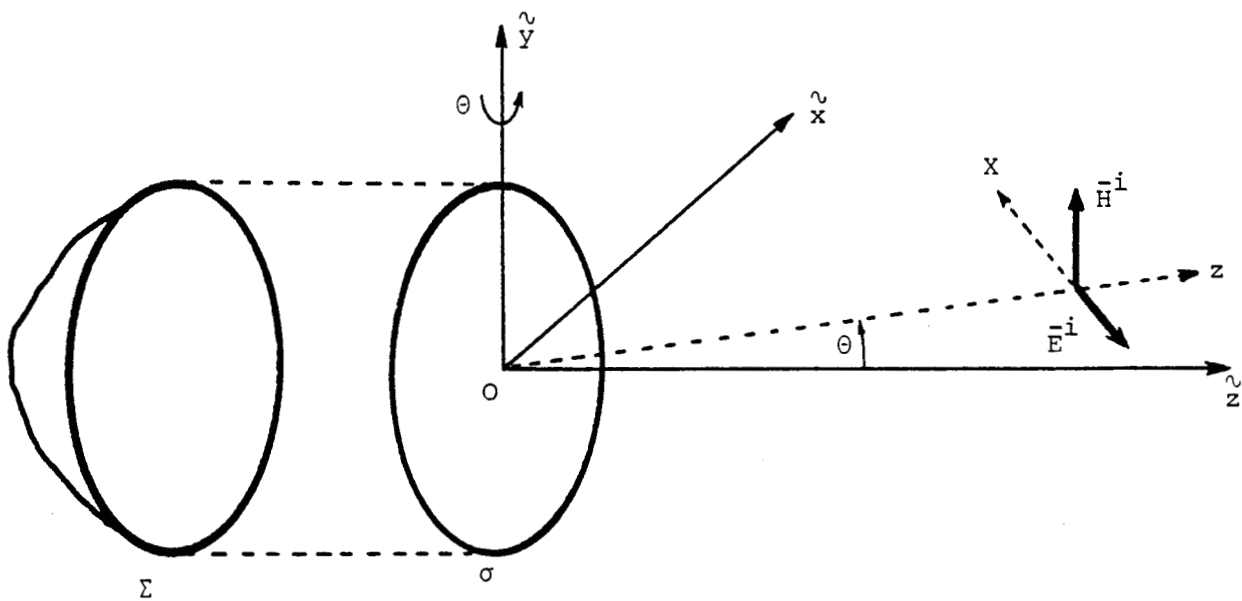


Figure 6. Geometry for example I (section on oblique incidence)

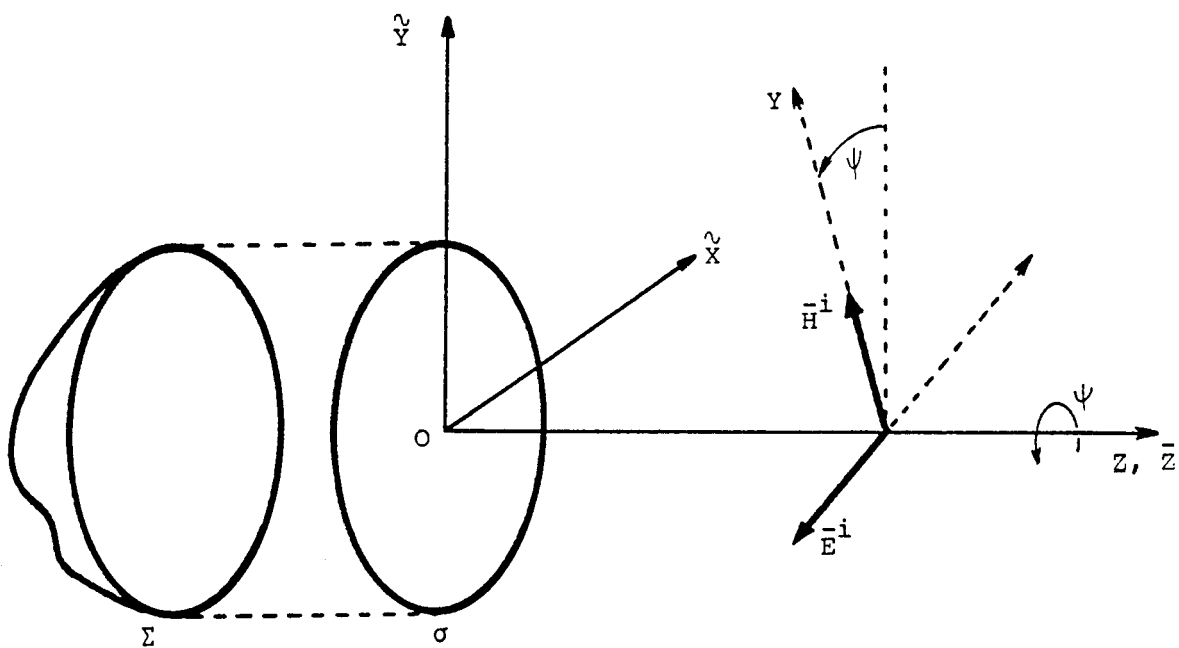


Figure 7. Geometry for example II (section on oblique incidence)

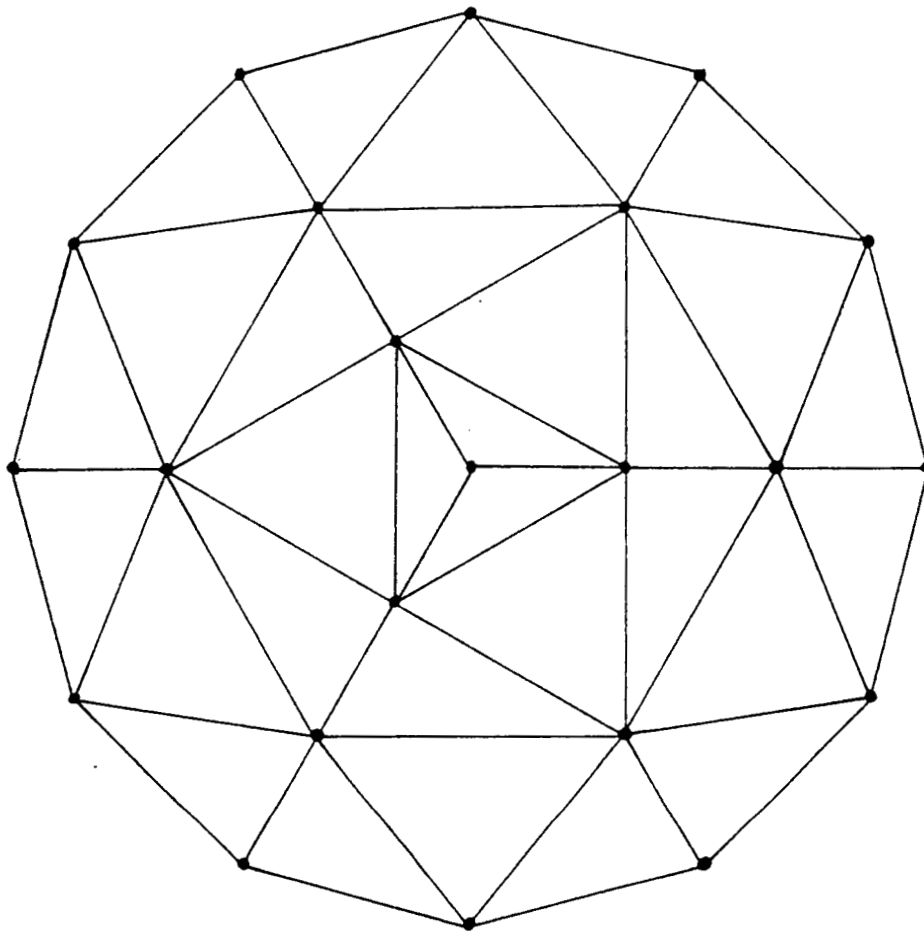


Figure 8. Discretization Scheme

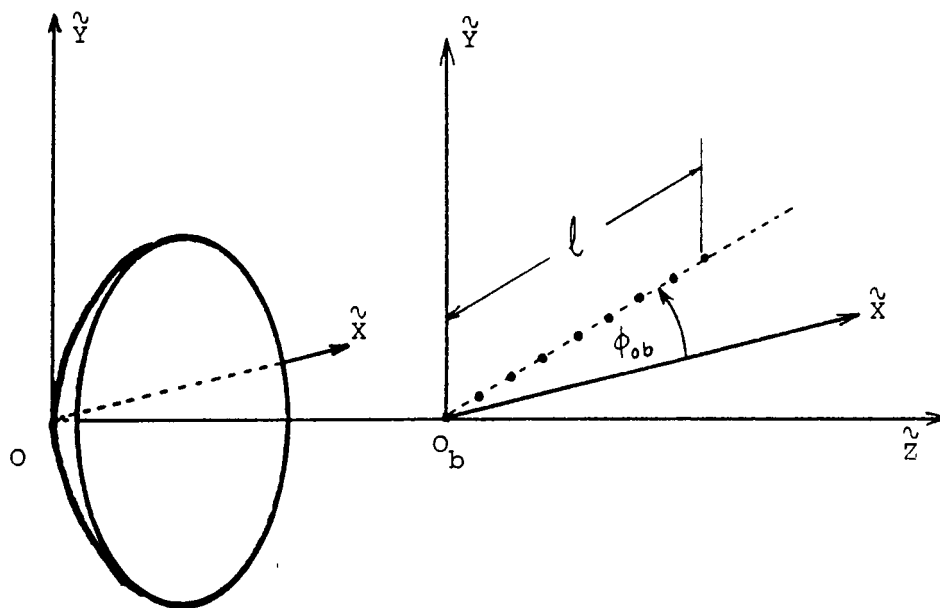


Figure 9. OO_b , ϕ_{ob} and l are the parameters used to define the distribution of the observation points

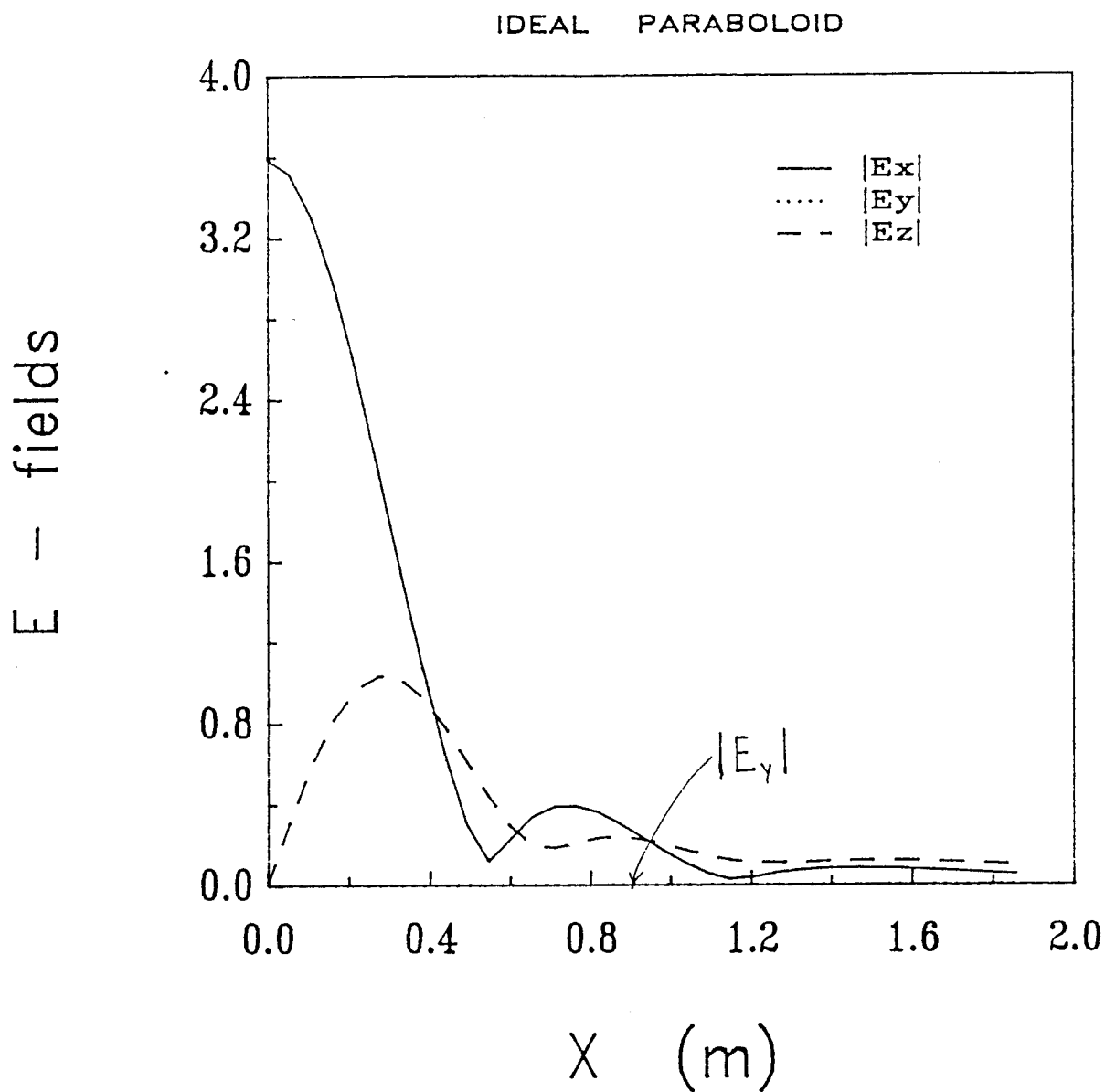


Figure 10. Normalized E . Observation points on the $0x$ axis.
 $f = 500$ MHz, $D = 2$ m, $F = 1.19$ m, $\beta\ell = 20$,
 $00_b = F$, $\theta = \phi = \psi = 0$. $A_1 = A_2 = A_3 = A_4 = 0$.

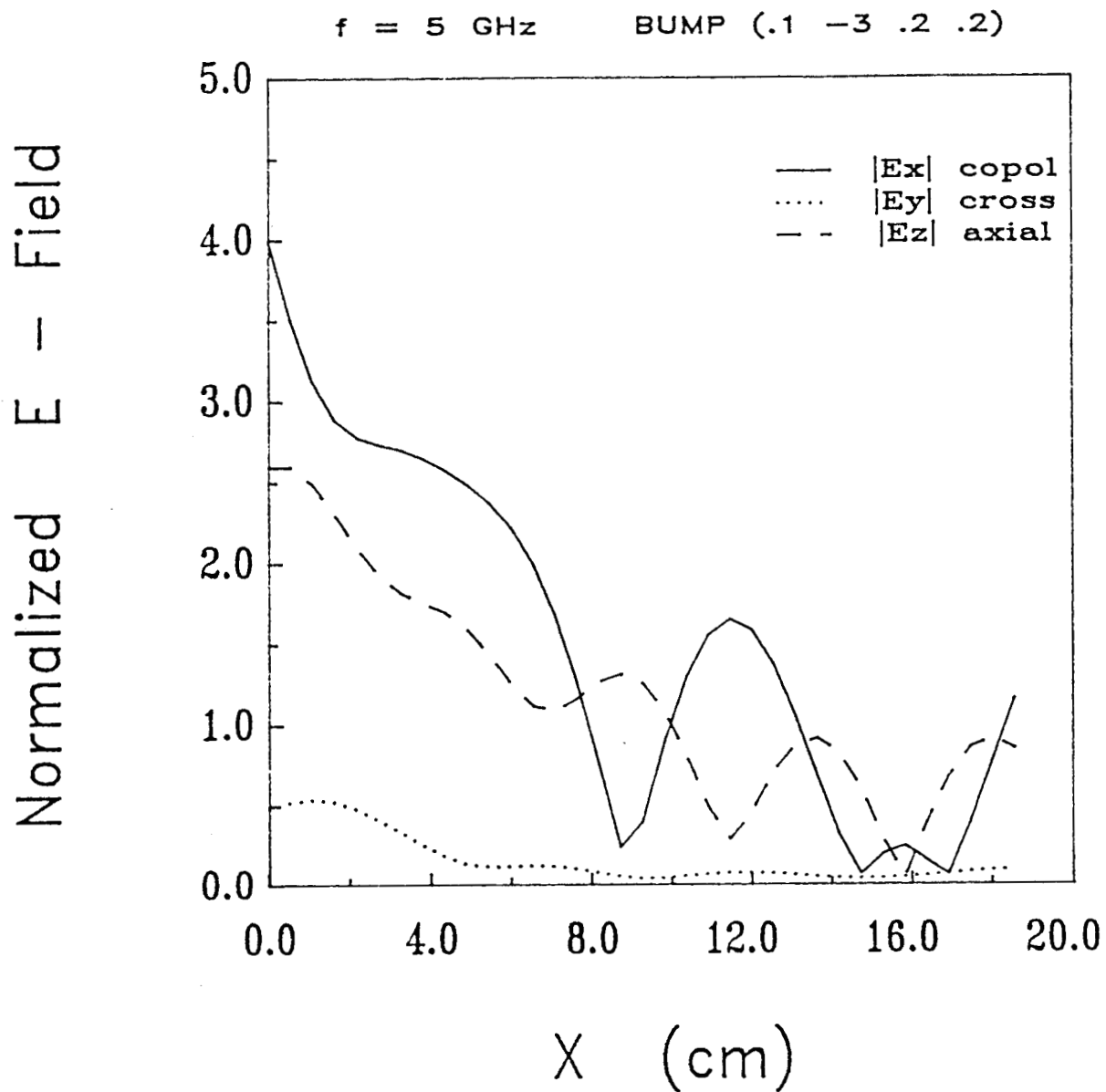


Figure 12. Normalized E . The distorted reflector of Figure 11 at $f = 5 \text{ GHz}$.

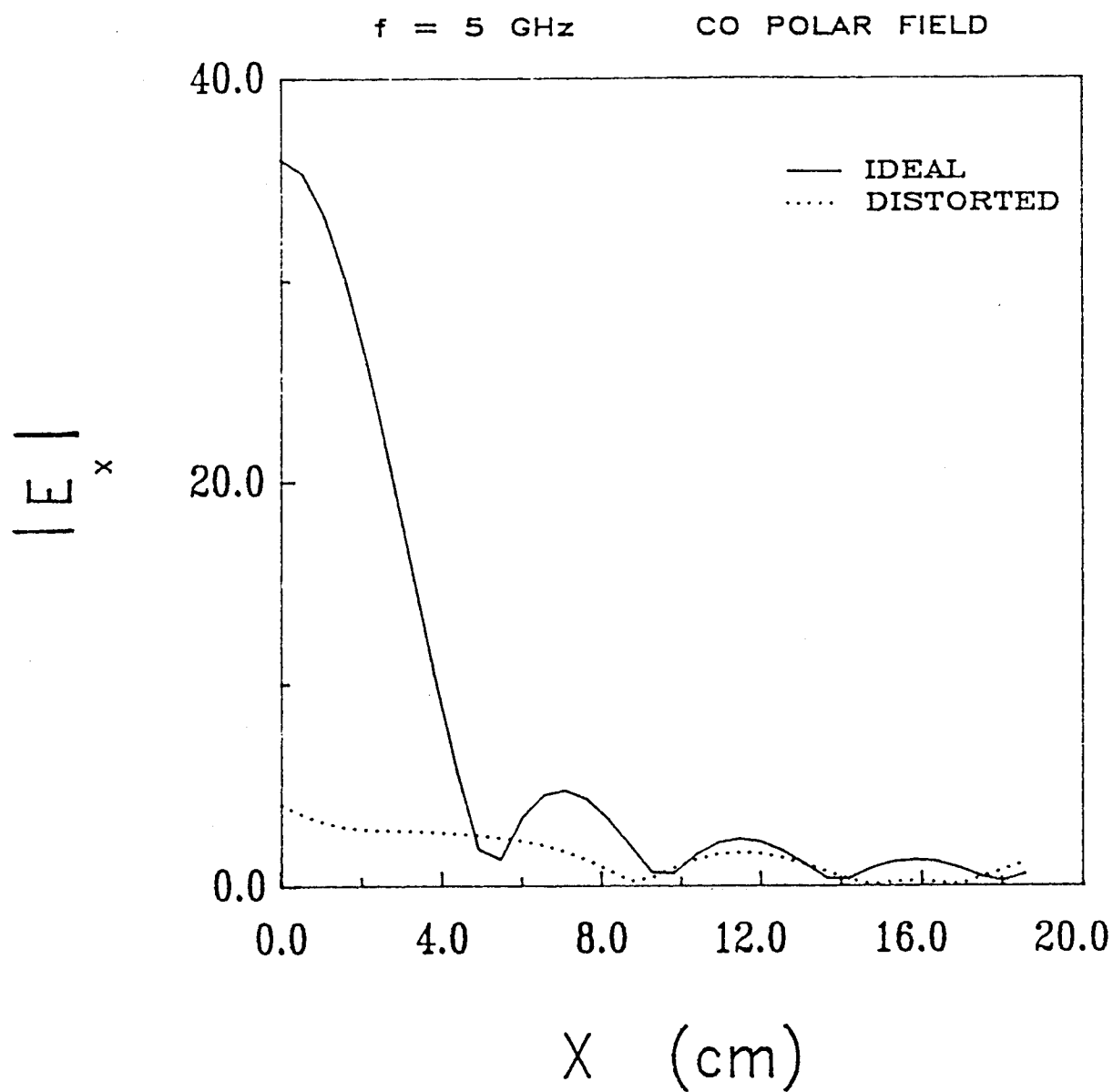


Figure 13a. Normalized $|E_x|$ of ideal and distorted reflectors.

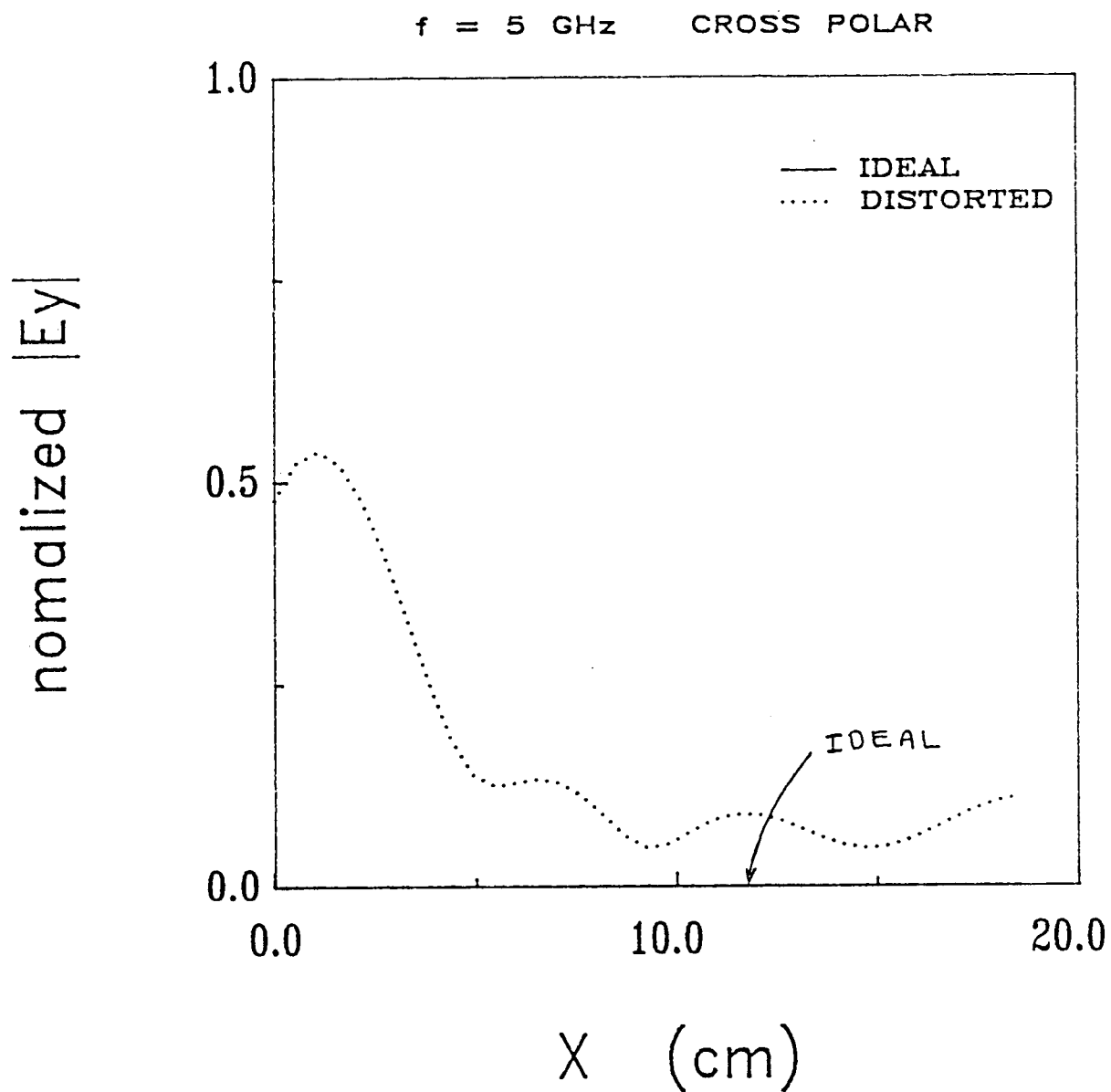


Figure 13b. Normalized $|E_y|$ of ideal and distorted reflectors.

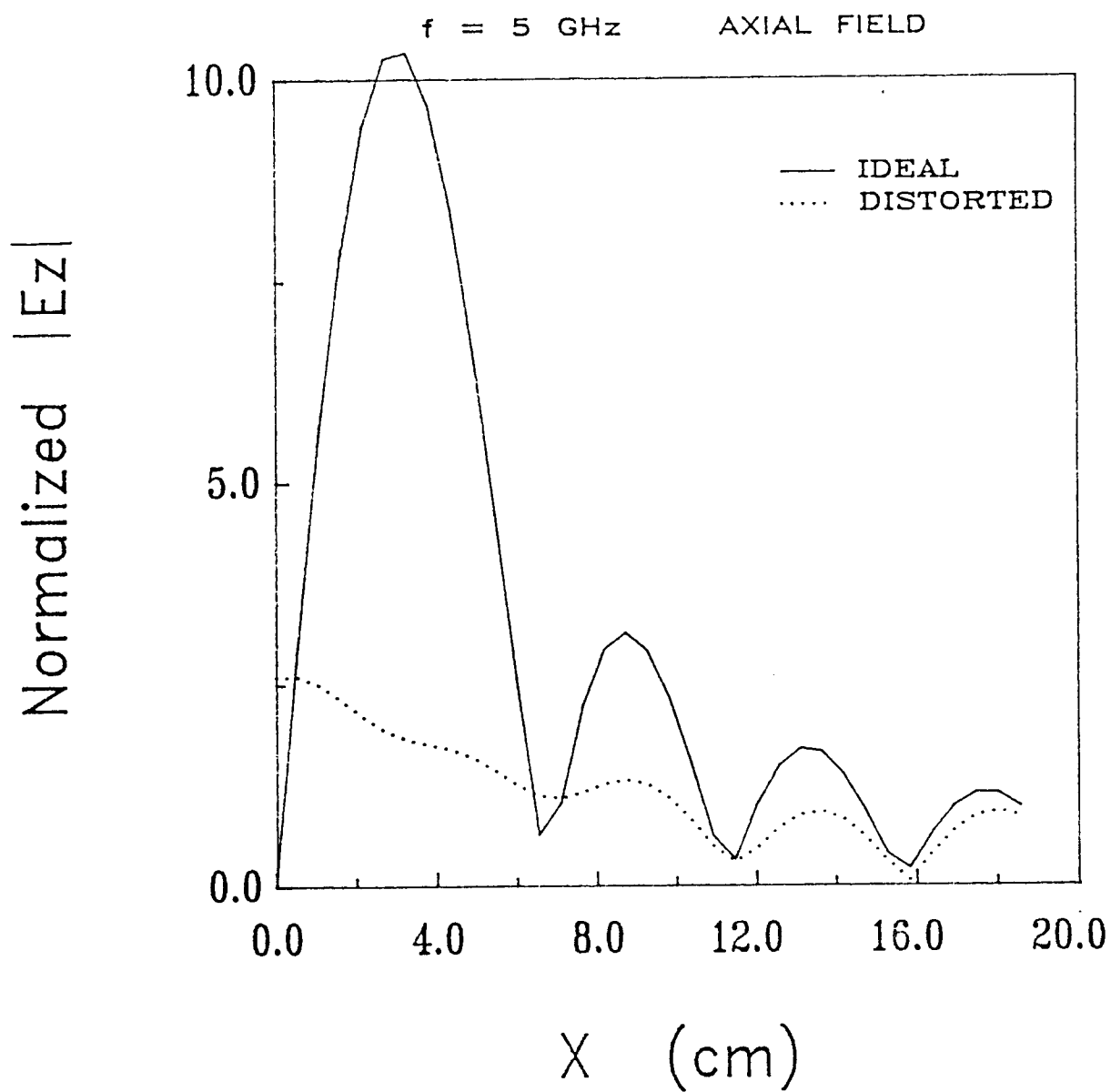


Figure 13c. Normalized $|E_z|$ of ideal and distorted reflectors.

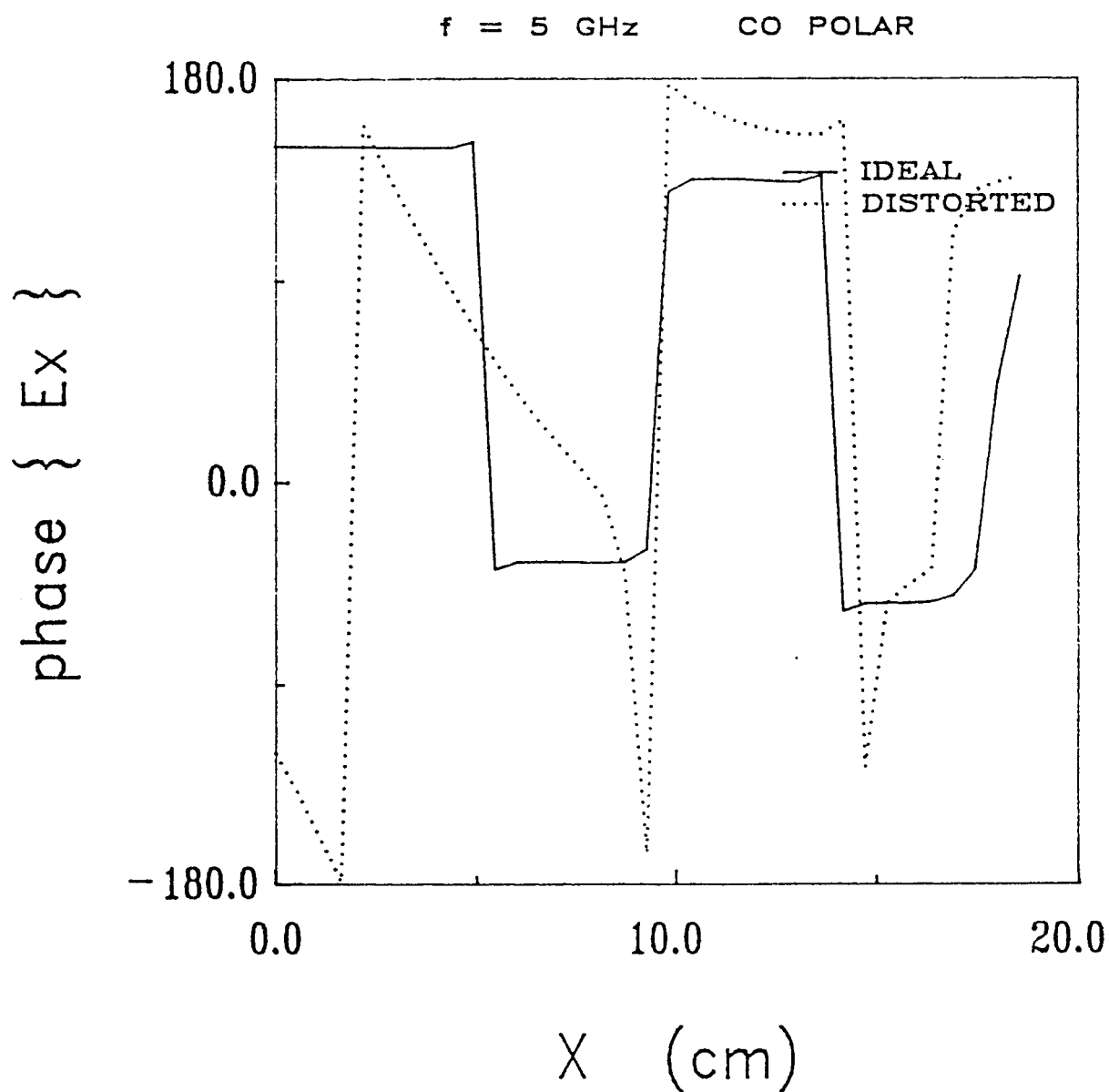


Figure 13d. Phase of coplanar component of ideal and distorted reflectors.

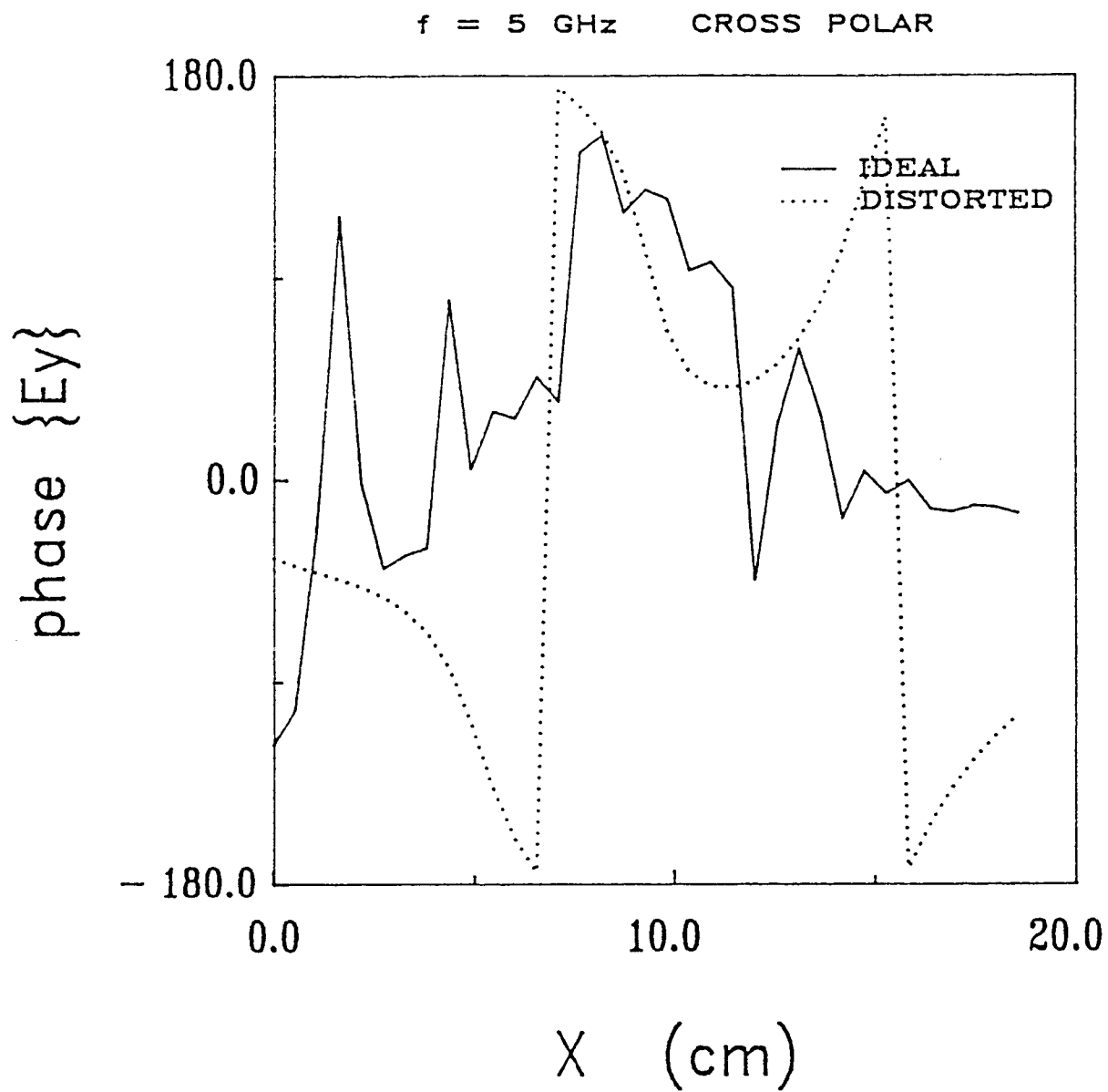


Figure 13e. Phase of cross-polar component of ideal and distorted reflectors.

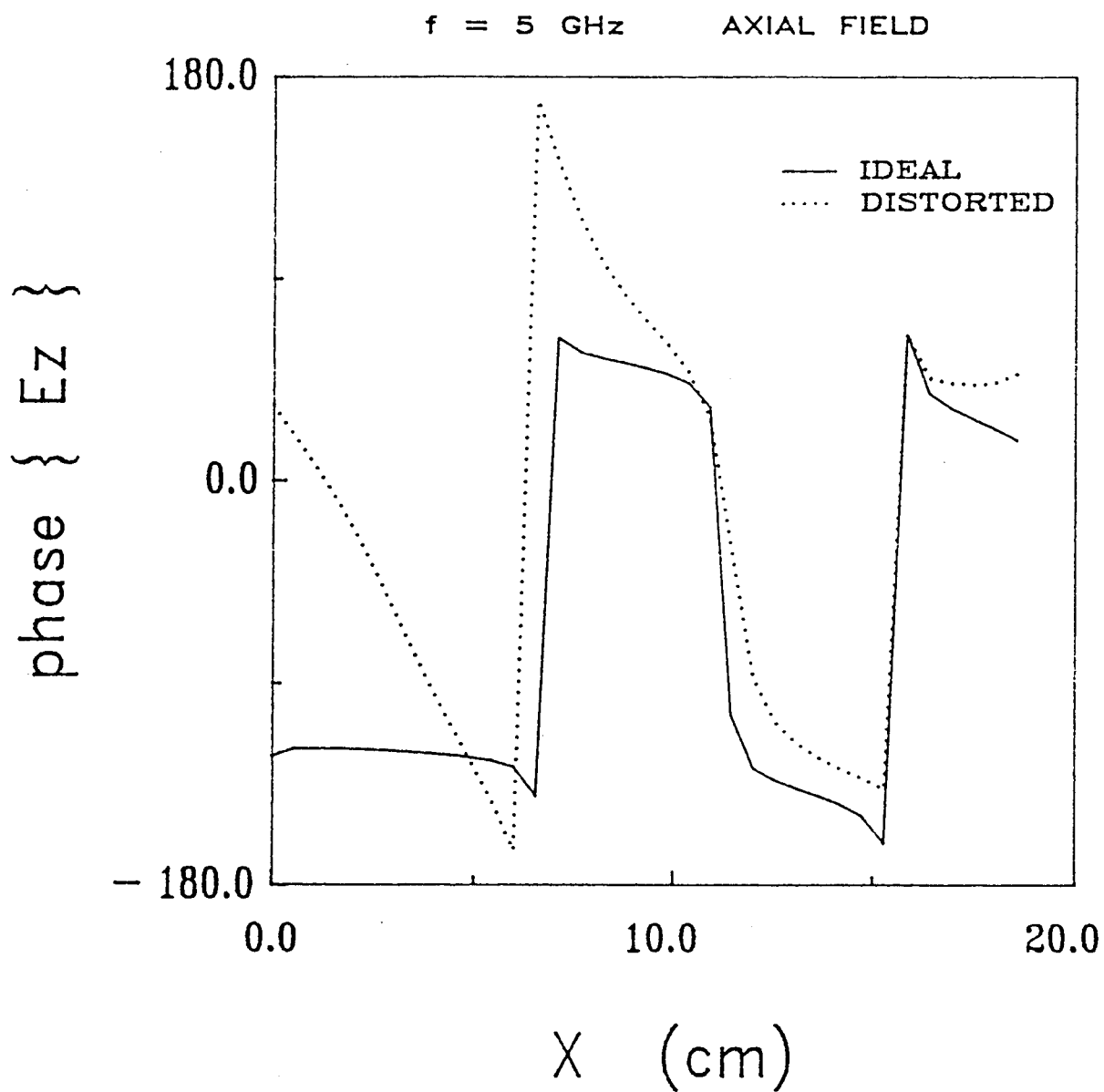


Figure 13f. Phase of axial component of ideal and distorted reflectors.

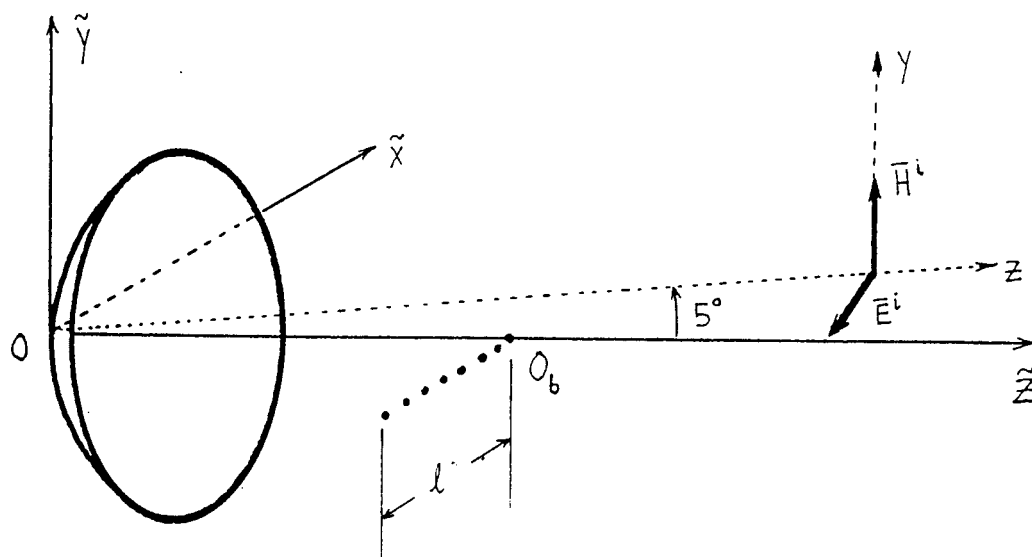


Figure 14. Oblique Incidence at $f = 5$ GHz. $\theta = 5^\circ$, $\phi = 0$, $\psi = 0$.
 $D = 2\text{m}$, $\beta l = 20$, $OO_b = F = 1.19\text{m}$.

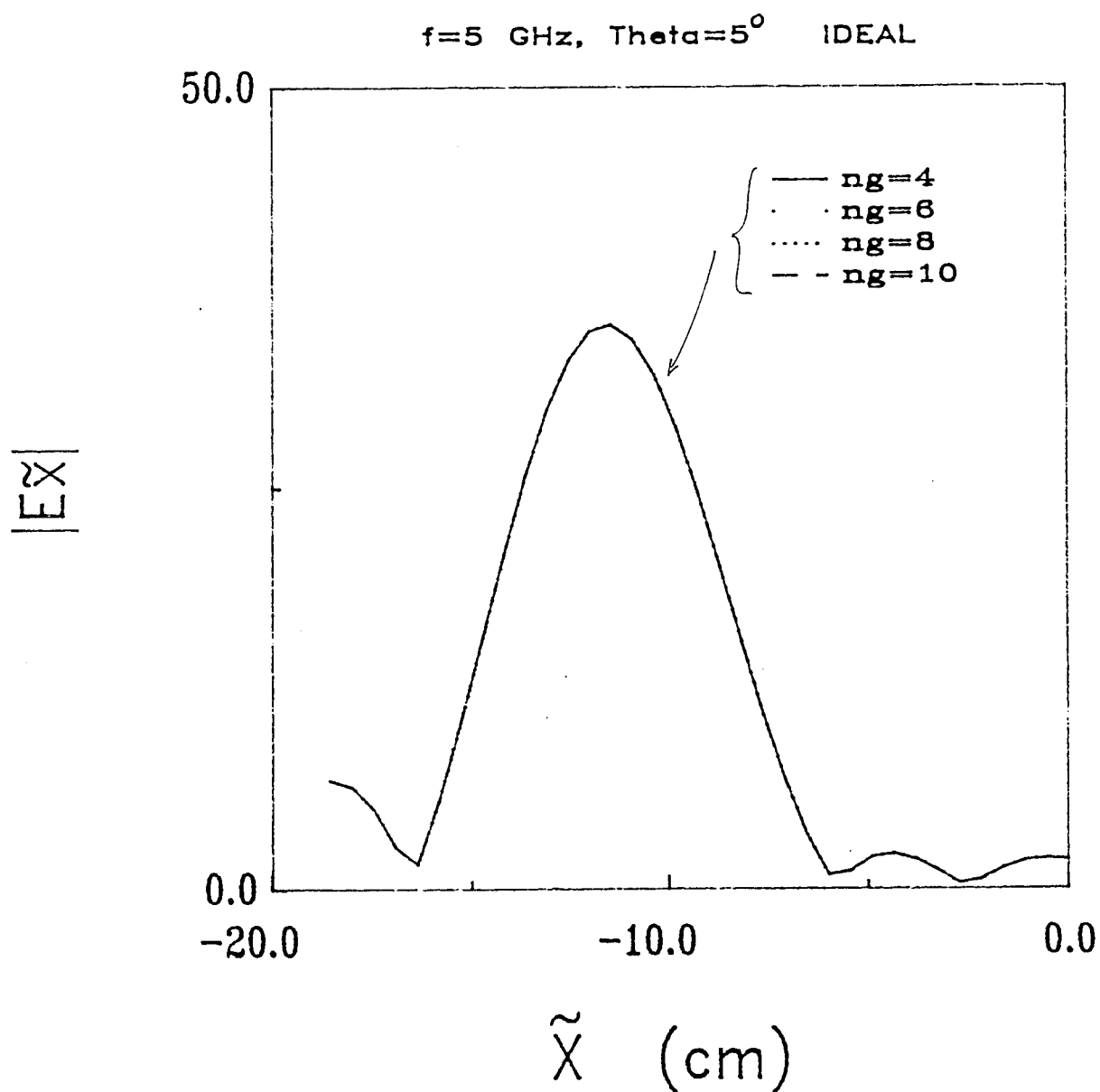


Figure 15. Normalized $|E\tilde{x}|$. Oblique incidence ($\theta = 5^\circ$, $\phi = 0$, $\psi = 0$).
 $D = 2\text{m}$, $F = 1.19\text{m}$, $A_1 = A_2 = A_3 = A_4 = 0$.

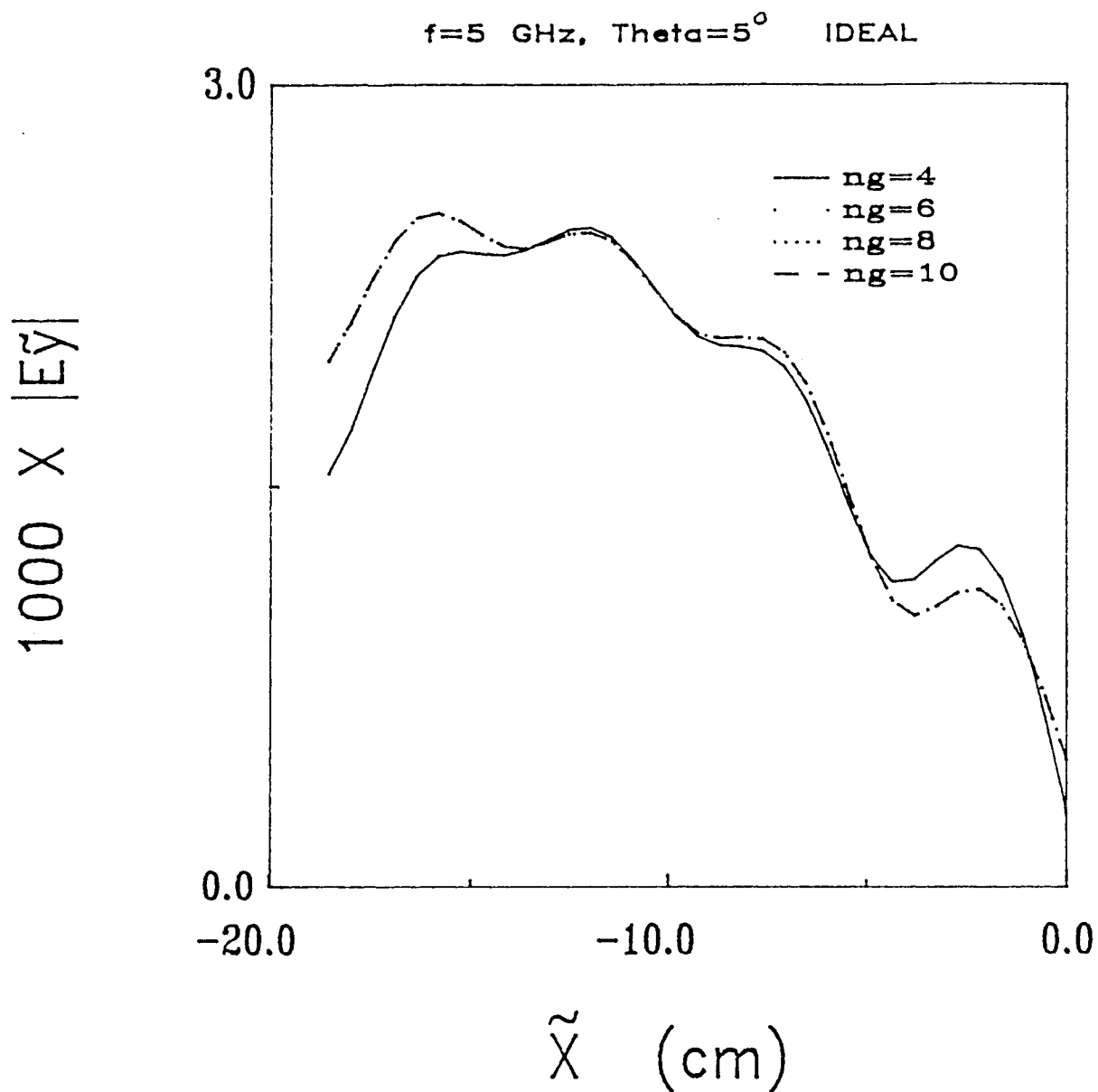


Figure 16. Normalized $|E_{\tilde{y}}|$. Oblique incidence ($\theta = 5^\circ, \phi = 0, \psi = 0$).
 $D = 2\text{m}, F = 1.19\text{m}, A_1 = A_2 = A_3 = A_4 = 0$.

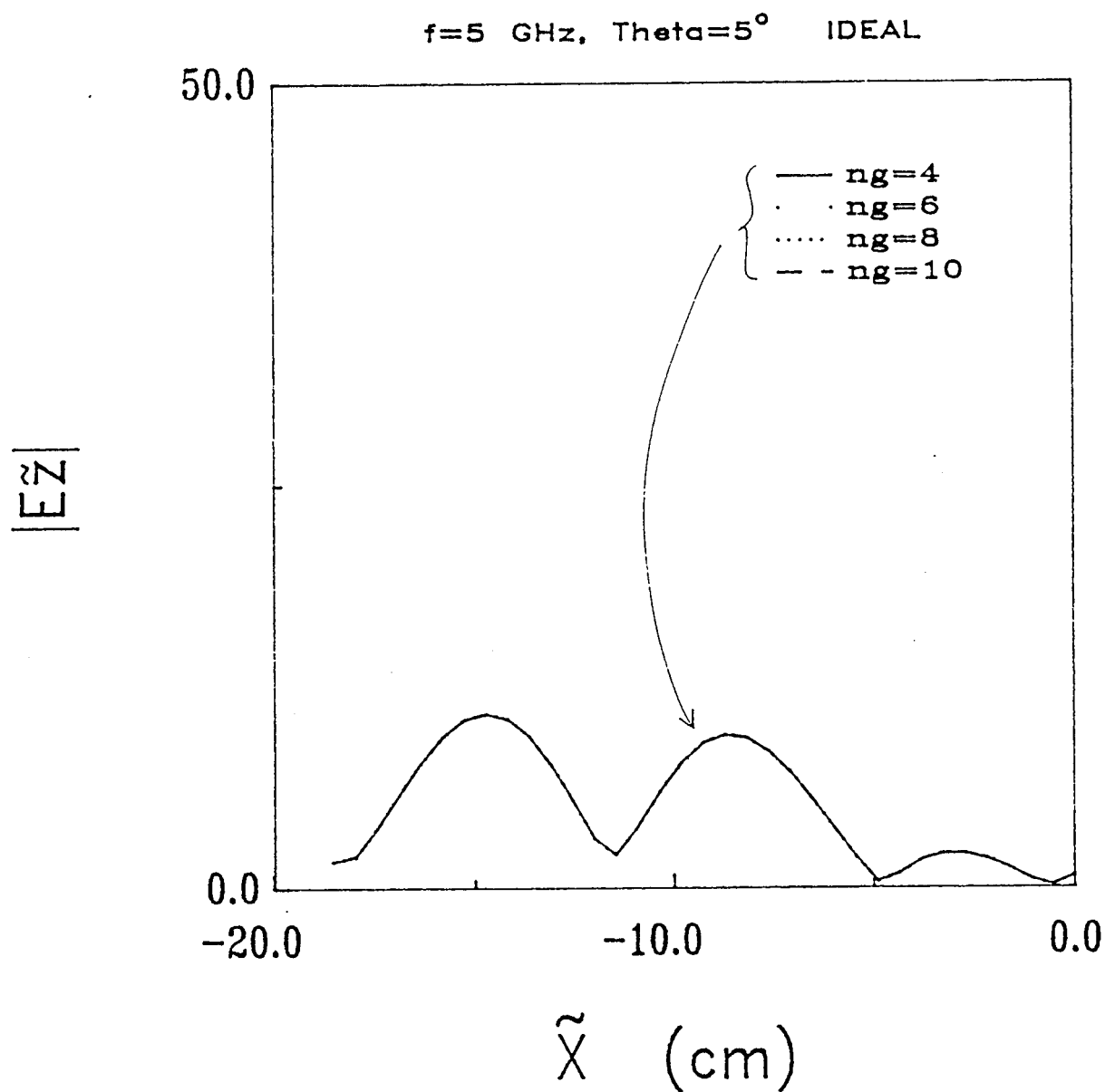


Figure 17. Normalized $|E\tilde{z}|$. Oblique incidence ($\theta = 5^\circ$, $\phi = 0$, $\psi = 0$).
 $D = 2\text{m}$, $F = 1.19\text{m}$, $A_1 = A_2 = A_3 = A_4 = 0$.

$\frac{|E_x|}{|E|}$

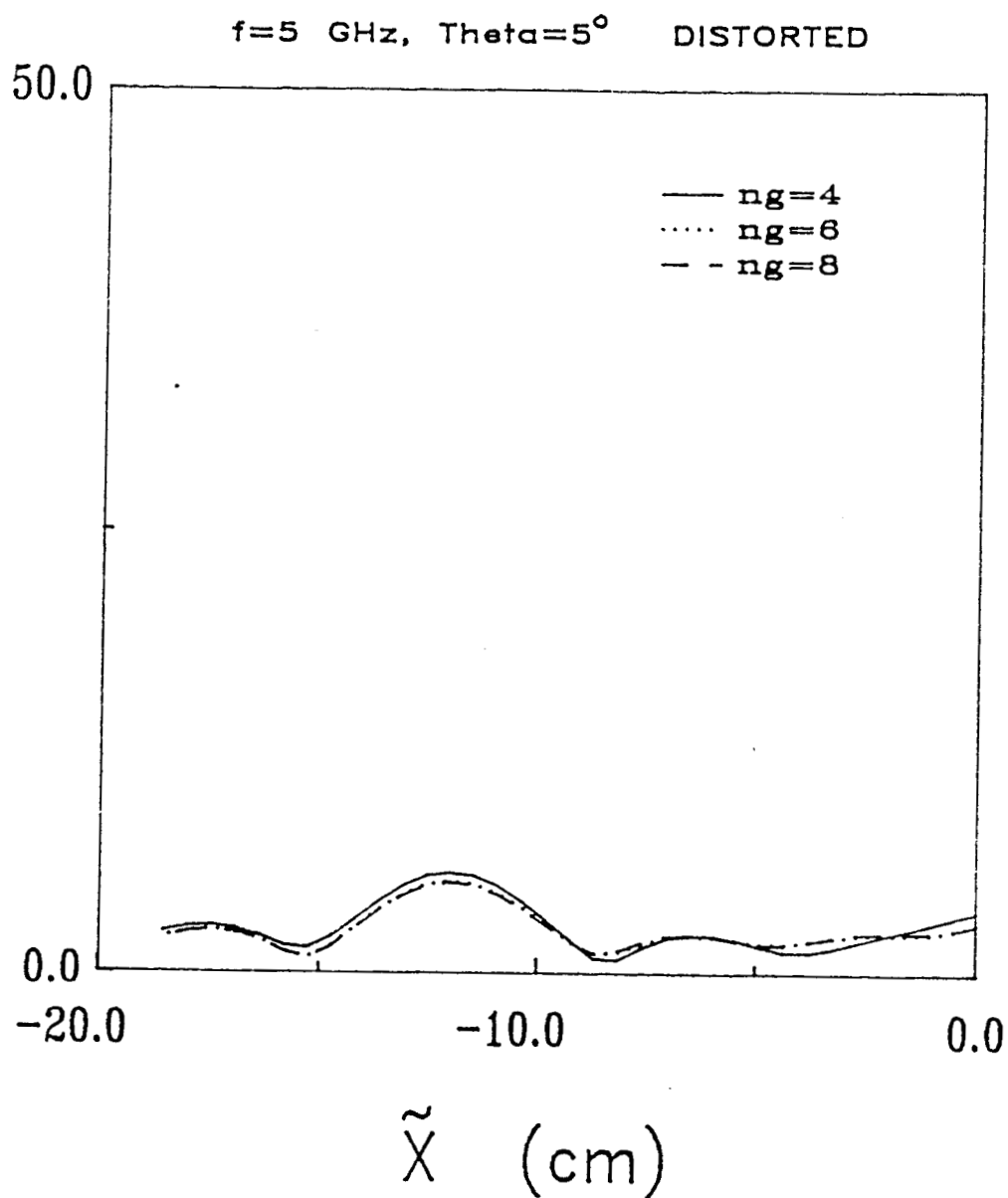


Figure 18. Normalized $|E\tilde{x}|$. Oblique incidence ($\theta = 5^\circ$, $\phi = \psi = 0$).
 $D = 2\text{m}$, $F = 1.19\text{m}$, $A_1 = 0.1\text{m}$, $A_2 = -3$, $A_3 = A_4 = 0$.

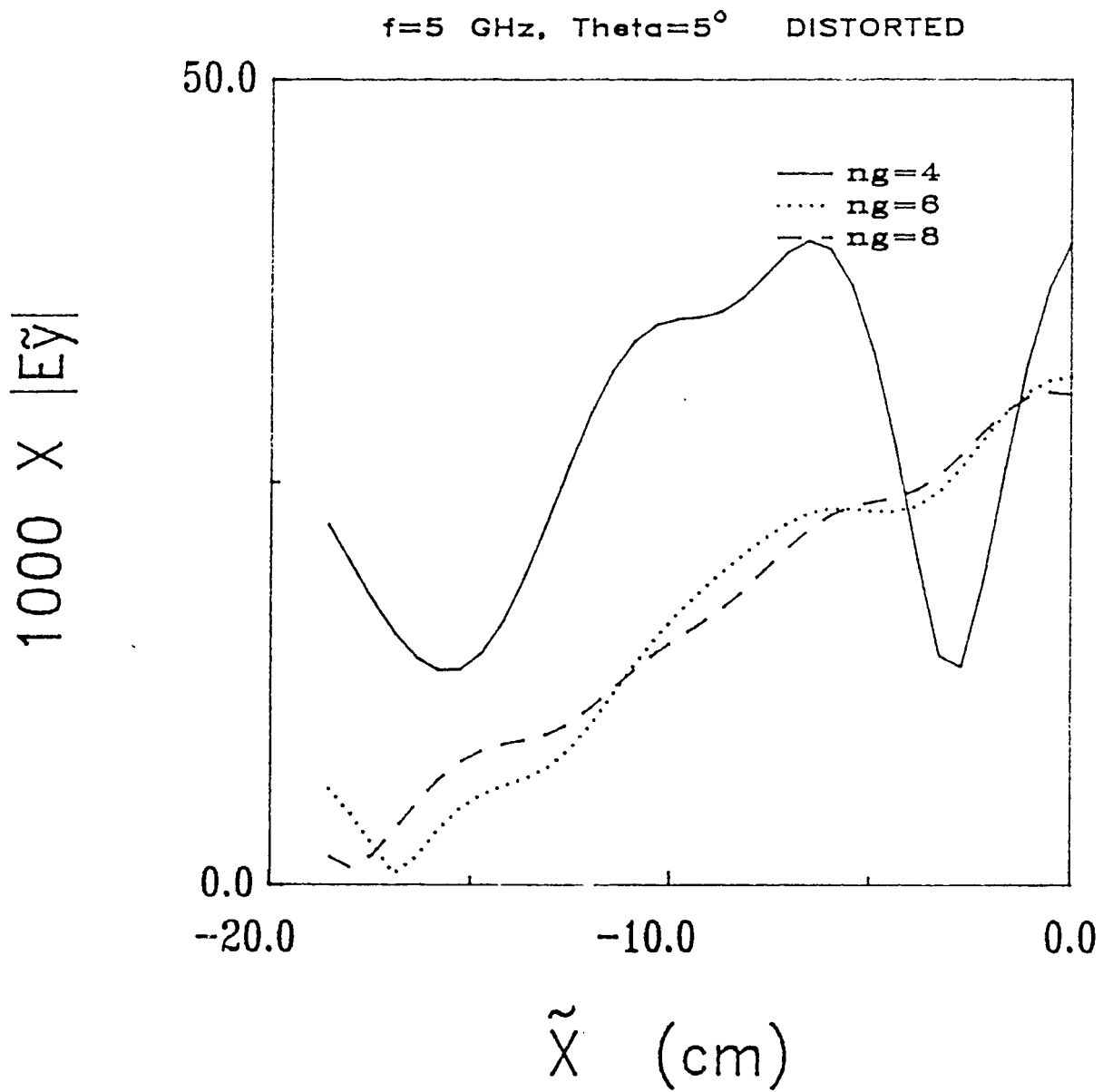


Figure 19. Normalized $|E_{\tilde{y}}|$. Oblique incidence ($\theta = 5^\circ$, $\phi = \psi = 0$).
 $D = 2\text{m}$, $F = 1.19\text{m}$, $A_1 = 0.1\text{m}$, $A_2 = -3$, $A_3 = A_4 = 0$.

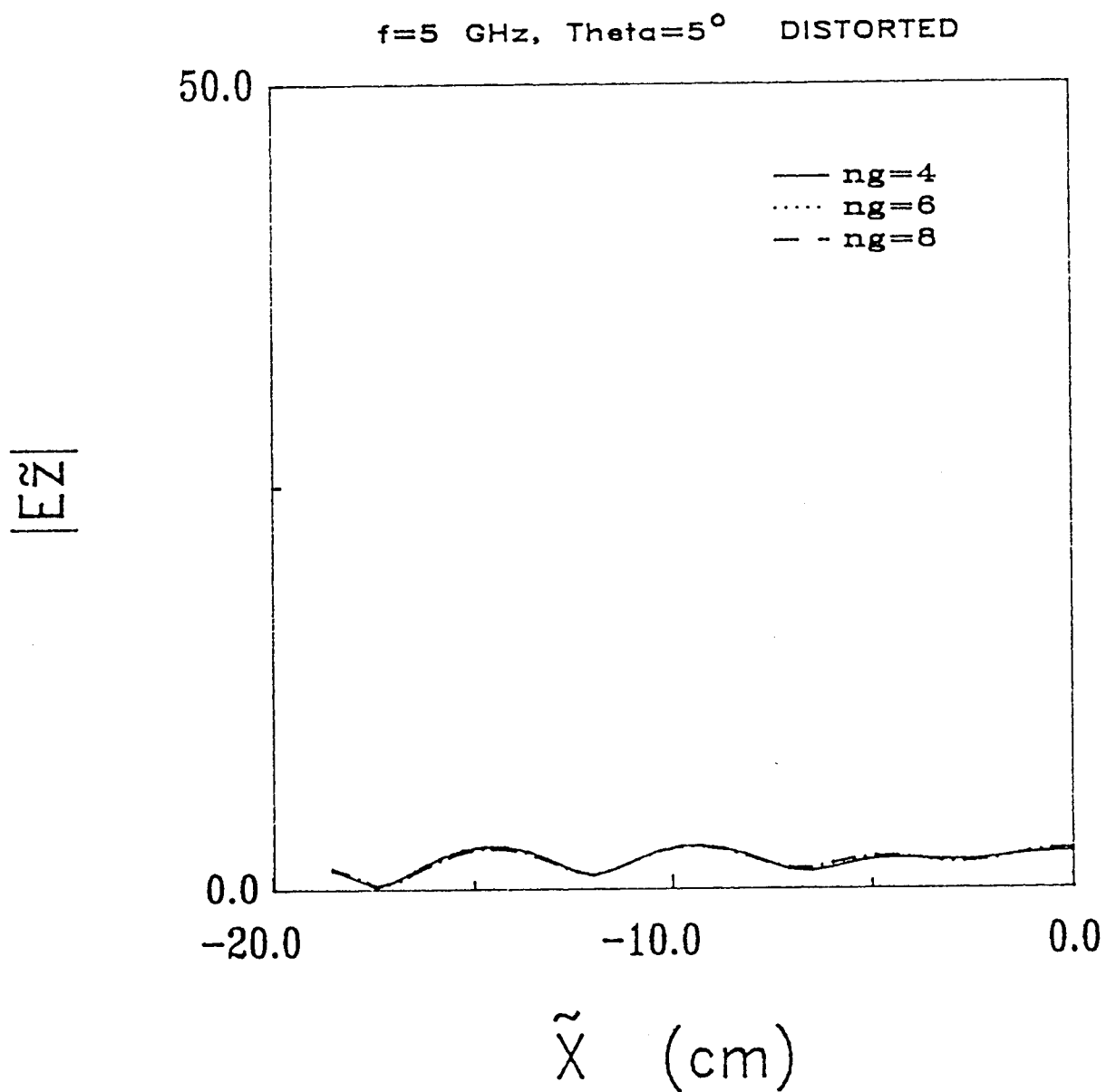


Figure 20. Normalized $|E\tilde{z}|$. Oblique incidence ($\theta = 5^\circ$, $\phi = \psi = 0$).
 $D = 2\text{m}$, $F = 1.19\text{m}$, $A_1 = 0.1\text{m}$, $A_2 = -3$, $A_3 = A_4 = 0$.

A

APPENDIX A

INSTRUCTIONS AND EXAMPLE OF CODE USAGE

FORTRAN SUBROUTINE JOORAN

SUBROUTINE JOORAN CALCULATES THE THREE COMPONENTS OF THE ELECTRIC FIELD SCATTERED FROM A PERFECT CONDUCTOR OF ARBITRARILY SHAPED SURFACE. THIS SURFACE IS SPECIFIED BY A SET OF TARGET POINTS. THE INCIDENT WAVE IS ASSUMED TO BE A PLANE WAVE WITH ORIENTATION DEFINED BY THREE EULERIAN ANGLES WITH RESPECT TO THE COORDINATE SYSTEM OF THE REFLECTOR. IT IS IMPORTANT TO MENTION THAT THE FIELD CALCULATED HERE IS NORMALIZED TO THE MAGNITUDE OF THE ELECTRIC FIELD OF THE INCIDENT WAVE. THE PLANE PERPENDICULAR TO THE DIRECTION OF PROPAGATION AND PASSES THROUGH THE ORIGIN IS THE ZERO PHASE PLANE. THE METHOD USED IS BASED ON A PHYSICAL OPTICS ANALYSIS. EDGE EFFECTS ARE INCLUDED IN THE SENSE THAT THE EFFECTS OF THE CHARGE AT THE BOUNDARY OF THE ILLUMINATED SURFACE OF THE REFLECTOR HAVE BEEN CONSIDERED (SEE SILVER "Microwave Antenna Theory and Design" section 5.8, Equations 62-69). FOR A DETAILED DESCRIPTION OF THE METHOD PLEASE, REFER TO THE REPORT ACCOMPANYING THIS SOURCE CODE. THIS CODE WAS DEVELOPED AT NORTH CAROLINA STATE UNIVERSITY BY DR. NICK E. BURIS AND DR. J. FRANK KAUFFMAN. SUPPORT FOR THIS STUDY WAS KINDLY OFFERED BY A NASA-LANGLEY RESEARCH CENTER GRANT. THIS CODE IS WRITTEN SO THAT IT CAN BE MODIFIED WITH THE MINIMUM POSSIBLE EFFORT. QUESTIONS ON THE OPERATION OF THIS CODE MAY BE ADDRESSED TO :

Nick E. Buris
University of Massachusetts
Dept. of Electrical and Computer Eng.
Marcus Hall Rm 20
Amherst, MA 01003
tel # (413) 545-2170

ATTENTION : ALL LENGTHS IN METERS, FREQUENCY in MHz.
SUBROUTINE JOORAN USES SUBROUTINE IBIRAN,
THEREFORE, WHEN COMPILING MAKE SURE THAT
YOU LINK TO A COMPILED VERSION OF IBIRAN.

ARGUMENT DESCRIPTION

INPUTS

nd	number of target points specifying the reflector (nd must be greater than 3)
xdtl	real array of dimension nd; (x coordinates of target points)
ydtl	real array of dimension nd; (y coordinates of target points)
zdtl	real array of dimension nd; (z coordinates of target points)
nob	number of observation points
xotl	real array of dimension nob; (x coordinates of

yotil observation points)
 real array of dimension nob; (y coordinates of
 observation points)
 zotil real array of dimension nob; (z coordinates of
 observation points)
 ald Eulerian angle theta in degrees
 a2d Eulerian angle phi in degrees
 a3d Eulerian angle psi in degrees
 freq real variable ; frequency in MHz
 ngauss integer variable that determines the density of
 points used in the Gaussian Quadrature method of
 numerical integration. The larger ngauss the better
 the approximation. Available ngauss=4,6,8,10,12,16,48.
 In the report, N and ng are used for ngauss.

OUTPUT

Estil Complex array of dimension (3,nob). It contains the
 values of the scattered Electric field.
 Estil(j,k) = j-th component of E at k-th observ. point
 j = 1 => Ex, j = 2 => Ey, j = 3 => Ez

WORK ARRAYS (OUTPUTS)

wk real array of dimension 14*nd
 iwk integer array of dimension 31*nd+1
 xd real array of dimension nd
 yd real array of dimension nd
 zd real array of dimension nd
 xob real array of dimension nob
 yob real array of dimension nob
 zob real array of dimension nob
 x real array of dimension (ngauss,ngauss)
 y real array of dimension (ngauss,ngauss)
 z real array of dimension (ngauss,ngauss)
 zx real array of dimension (ngauss,ngauss)
 Ro real array of dimension (ngauss,ngauss)
 SCA1 complex array of dimension (ngauss,ngauss)
 SCA2 complex array of dimension (ngauss,ngauss)
 SCA3 complex array of dimension (ngauss,ngauss)
 gw double precision real array of dimension ngauss
 gz double precision real array of dimension ngauss
 u real array of dimension ngauss
 v real array of dimension (ngauss,ngauss)

TO USE JOORAN SIMPLY CALL IT WITH A CALL STATEMENT LIKE

```

call Jooran(nd,xdtl,ydtl,zdtl,nob,xotil,yotil,zotil,
1          ald,a2d,a3d,freq,ngauss,Estil,
2  wk,iwk,xd,yd,zd,xob,yob,zob,x,y,z,zx,Ro,SCA1,SCA2,SCA3,
3  gw,gz,u,v)
  
```

The first two lines of arguments contain the input arguments and the output argument Estil. The last two lines of arguments contain work arrays. The general user need not worry about these arrays. However, if changes in the program are needed for extensions and/or modifications, then the user should consult the theoretical part of this report and keep in mind that :

- 1) x_d, y_d and z_d are the coordinates of the target points in the ray system (OXYZ).
- 2) x_{ob}, y_{ob} and z_{ob} are the coordinates of the observation points in the ray system (OXYZ).
- 3) x, y, z, z_x contain the values of x, y, z and Z_x at the points defined by the grid n_{gauss} X n_{gauss} on each individual triangle. These values are used in the numerical integration scheme.
- 4) R_o contains the values of the distance of the current observation point from each of the point of the grid mentioned in 3.
- 5) $SCA1, SCA2$ and $SCA3$ contain some common factors that appear in the integral expressions for all the three components of the Electric field. Again, these values are calculated at the points of the grid mentioned in 3.
- 6) g_w, g_z are the weights and the zeros of Legendre polynomials used in the Gaussian Quadrature integration.
- 7) u, v are the coordinates of the points of the grid mentioned in 3 expressed in the $u-v$ coordinate system. In this coordinate system all the individual triangles are mapped onto a basic triangle.

As an example of using Jooran consider the following data file

NASA87.DAT

```

5000.000          frequency in MHz
                    4  one of (4,6,8,10,12,16,48)
5.000000          0.000000E+00  0.000000E+00  Euler angles
                    22 # of target points
0.0000000000000000E+00  0.0000000000000000E+00  0.0000000000000000E+00
0.3333333333333333  0.0000000000000000E+00  2.1367522151277409E-02
-0.1666666666666667  0.2886751345948129  2.1367522151277410E-02
-0.1666666666666667  -0.2886751345948129  2.1367522151277409E-02
0.6666666666666667  0.0000000000000000E+00  8.5470088605109637E-02
0.3333333333333333  0.5773502691896258  8.5470088605109636E-02
-0.3333333333333333  0.5773502691896258  8.5470088605109639E-02
-0.6666666666666667  -2.9379182519358776E-17  8.5470088605109637E-02
-0.3333333333333333  -0.5773502691896258  8.5470088605109637E-02
0.3333333333333333  -0.5773502691896258  8.5470088605109639E-02
1.0000000000000000  0.0000000000000000E+00  0.1923076993614967
0.8660254037844387  0.5000000000000000  0.1923076993614967
0.5000000000000000  0.8660254037844386  0.1923076993614967
-2.2034386889519082E-17  1.0000000000000000  0.1923076993614967
-0.5000000000000000  0.8660254037844387  0.1923076993614967
-0.8660254037844386  0.5000000000000000  0.1923076993614967
-1.0000000000000000  -4.4068773779038163E-17  0.1923076993614967
-0.8660254037844387  -0.5000000000000000  0.1923076993614967
-0.5000000000000000  -0.8660254037844386  0.1923076993614967
-7.2674717409587322E-17  -1.0000000000000000  0.1923076993614967
0.5000000000000000  -0.8660254037844387  0.1923076993614967
0.8660254037844386  -0.5000000000000000  0.1923076993614967
2 (nob # of observation points)
0.0000000000000000E+00  0.0000000000000000E+00  1.299999952316284
4.7746483236551285E-02  0.0000000000000000E+00  1.299999952316284

```

This data file, nasa87.dat, is input to the following program :

```

real xdtil(200),ydtil(200),zdtil(200)
real xotil(50),yotil(50),zotil(50)
real xd(200),yd(200),zd(200),wk(14*200)
real Xob(50),Yob(50),Zob(50)
complex Estil(3,50)
integer nd,iwk(31*200+1*1)

real x(48,48),y(48,48),z(48,48)
real zx(48,48)
real Ro(48,48)

complex SCA1(48,48),SCA2(48,48)
complex SCA3(48,48)
dimension gw(48),gz(48),u(48),v(48,48)
double precision gw,gz

open(1,file='nasa87.dat')
read(1,*)freq
read(1,*)ngauss
read(1,*)ald,a2d,a3d
read(1,*)nd
do 1 k=1,nd
  read(1,*)xdtil(k),ydtil(k),zdtil(k)
1 continue
  read(1,*)nob
  do 2 k=1,nob
    read(1,*)xotil(k),yotil(k),zotil(k)
  2 continue

  call Jooran(nd,xdtil,ydtil,zdtil,nob,xotil,yotil,zotil,
1      ald,a2d,a3d,freq,ngauss,Estil,
2      wk,iwk,xd,yd,zd,xob,yob,zob,x,y,z,zx,Ro,SCA1,SCA2,SCA3,
3      gw,gz,u,v)

open(2,file='nasout.dat')
write(2,*)'      ',nob,'      # of observation points'
do 3 k=1,nob
  write(2,*)'      ',xotil(k),',',yotil(k),
$',',zotil(k),',      Xotil,Yotil,Zotil'
  write(2,*)'      ',Estil(1,k),'Ext'il'
  write(2,*)'      ',Estil(2,k),'Eyt'il'
  write(2,*)'      ',Estil(3,k),'Ezt'il'
3 continue
stop
end

```

The output is sent to the file "nasout.dat"

NASOUT.DAT

```
      2  # of observation points
0.0000000E+00, 0.0000000E+00, 1.300000 Xotil,Yotil,Zotil
(-1.501289,-0.8454167)Exttil
(-7.9167667E-06,1.5168914E-04)Eytil
(0.2458099,-0.5834020)Eztil
4.7746483E-02, 0.0000000E+00, 1.300000 Xotil,Yotil,Zotil
(0.6274602,0.1810894)Exttil
(-1.3166843E-03,-4.8433035E-04)Eytil
(-0.1880506,0.5139895)Eztil
```

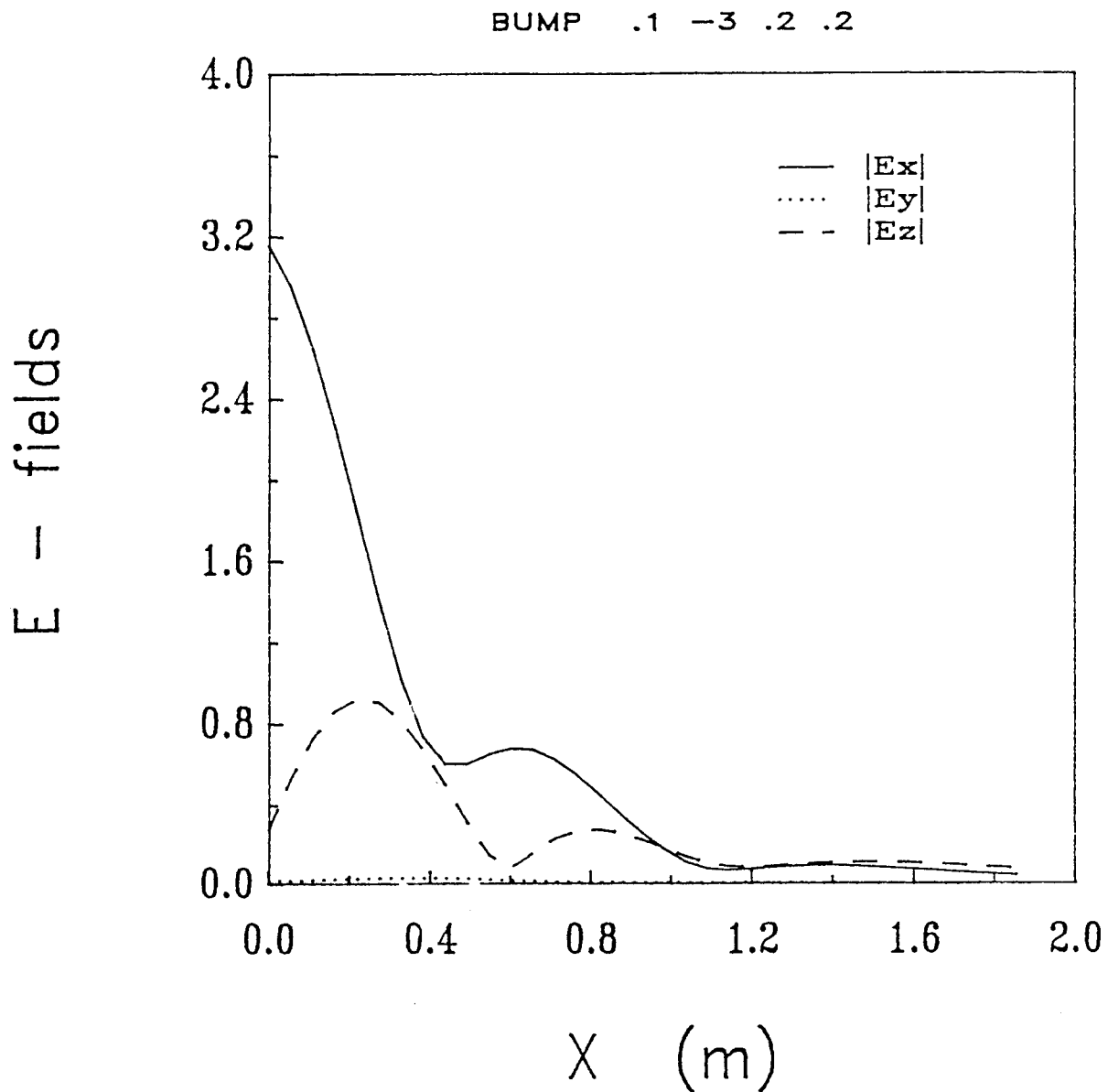


Figure 11. Normalized E . Observation points on the $0x$ axis.
 $f = 500 \text{ MHz}$, $D = ?\text{m}$, $F = 1.19\text{m}$, $\beta\ell = 20$,
 $00_b = F$, $\theta = \phi = \psi = 0$. $A_1 = 0.1\text{m}$, $A_2 = -3$, $A_3 = 0.2\text{m}$, $A_4 = 0.2\text{m}$.

APPENDIX B

SUBROUTINE JOORAN FORTRAN CODE

```

C*****
C  THE FOLLOWING SUBROUTINE CALCULATES THE THREE COMPONENTS OF THE *
C  ELECTRIC FIELD SCATTERED FROM AN ARBITRARY PERFECT CONDUCTOR . *
C  THE INCIDENT WAVE IS ASSUMED TO BE A PLANE WAVE WITH ORIENTATION*
C  DEFINED BY THREE EULERIAN ANGLES WITH RESPECT TO THE OPTICAL    *
C  AXIS OF THE REFLECTOR. IT IS IMPORTANT TO NOTE THAT THE FIELDS *
C  ARE NORMALIZED TO THE MAGNITUDE OF THE ELECTRIC FIELD OF THE    *
C  INCIDENT WAVE. THE PLANE PERPENDICULAR TO THE DIRECTION OF PRO- *
C  PAGATION AND PASSES THROUGH THE ORIGIN IS THE ZERO PHASE PLANE. *
C  THE METHOD USED IS BASED ON A PHYSICAL OPTICS ANALYSIS AND EDGE *
C  EFFECTS ARE INCLUDED. FOR A DETAILED DESCRIPTION OF THE METHOD, *
C  PLEASE REFER TO THE REPORT ACCOMPANYING THIS SOURCE CODE .      *
C  THIS CODE WAS DEVELOPED AT NORTH CAROLINA STATE UNIVERSITY BY   *
C  DR. NICK E. BURIS AND DR. J. FRANK KAUFFMAN . SUPPORT FOR      *
C  THIS STUDY WAS KINDLY OFFERED BY A NASA-LANGLEY RESEARCH CENTER *
C  GRANT.                                                           *
C  THIS CODE IS WRITTEN SO THAT IT CAN BE MODIFIED WITH THE MINIMUM*
C  POSSIBLE EFFORT.                                                *
C                                                                    *
C                                                                    *
C  ARGUMENT DESCRIPTION                                           *
C  ~~~~~~                                                         *
C                                                                    *
C                                INPUTS                            *
C                                                                    *
C  nd          number of target points defining the reflector    *
C  xdtil       real array of dimension nd; (x coordinates of      *
C              target points)                                     *
C  ydtil       real array of dimension nd; (y coordinates of      *
C              target points)                                     *
C  zdtil       real array of dimension nd; (z coordinates of      *
C              target points)                                     *
C  nob         number of observation points                       *
C  xotil       real array of dimension nob; (x coordinates of     *
C              observation points)                                *
C  yotil       real array of dimension nob; (y coordinates of     *
C              observation points)                                *
C  zotil       real array of dimension nob; (z coordinates of     *
C              observation points)                                *
C  ald         Eulerian angle theta in degrees                   *
C  a2d         Eulerian angle phi in degrees                     *
C  a3d         Eulerian angle alpha in degrees                   *
C  freq        real variable ; frequency in MHz                  *
C  ngauss      integer variable that determines the density of   *
C              points used in the Gaussian Quadrature method of  *
C              numerical integration. The larger ngauss the better *
C              the approximation. Available ngauss=4,6,8,10,12,16,48.*
C                                                                    *
C                                OUTPUT                             *
C  Estil       Complex array of dimension (3,nob). It contains the *
C              values of the scattered Electric field.           *
C              Estil(j,k) = j-th component of E at k-th observ. point*
C              j = 1 => Ex,    j = 2 => Ey,    j = 3 => Ez        *
C                                                                    *
C                                WORK ARRAYS                       *
C  wk          real array of dimension 14*nd                      *

```

```

C      iwkw      integer array of dimension 31*nd+1      *
C      xd        real array of dimension nd              *
C      yd        real array of dimension nd              *
C      zd        real array of dimension nd              *
C      xob       real array of dimension nob              *
C      yob       real array of dimension nob              *
C      zob       real array of dimension nob              *
C      x         real array of dimension (ngauss,ngauss) *
C      y         real array of dimension (ngauss,ngauss) *
C      z         real array of dimension (ngauss,ngauss) *
C      zx        real array of dimension (ngauss,ngauss) *
C      Ro        real array of dimension (ngauss,ngauss) *
C      SCA1      complex array of dimension (ngauss,ngauss) *
C      SCA2      complex array of dimension (ngauss,ngauss) *
C      SCA3      complex array of dimension (ngauss,ngauss) *
C      gw        double precision real array of dimension ngauss *
C      gz        double precision real array of dimension ngauss *
C      u         real array of dimension ngauss          *
C      v         real array of dimension (ngauss,ngauss) *
C
C*****
      subroutine Jooran(nd,xdtil,ydtil,zdtil,nob,xotil,yotil,zotil,
1         ald,a2d,a3d,freq,ngauss,Estil,
2         wk,iwk,xd,yd,zd,xob,yob,zob,x,y,z,zx,Ro,SCA1,SCA2,SCA3,
3         gw,gz,u,v)
      real xdtil(nd),ydtil(nd),zdtil(nd)
      real xotil(nob),yotil(nob),zotil(nob)
      real xd(nd),yd(nd),zd(nd),xi,yi,zi,wk(14*nd)
      real Xob(nob),Yob(nob),Zob(nob)
      complex Estil(3,nob)
      integer nd,iop(2),iwk(31*nd+1*1),ierr,nxi,nyi

      real x(ngauss,ngauss),y(ngauss,ngauss),z(ngauss,ngauss)
      real zx(ngauss,ngauss)
      real Ro(ngauss,ngauss)
      complex SCA1(ngauss,ngauss),SCA2(ngauss,ngauss)
      complex SCA3(ngauss,ngauss)
      dimension gw(ngauss),gz(ngauss),u(ngauss),v(ngauss,ngauss)
      double precision gw,gz
      common /observ/ Xo,Yo,Zo,beta
      COMMON /IBCDPT/ X0,Y0,AP,BP,CP,DP,P00,P10,P20,P30,P40,P50,
1         P01,P11,P21,P31,P41,P02,P12,P22,P32,P03,P13,
2         P23,P04,P14,P05,ITPV

      common /vertex/ x1,x2,x3,y1,y2,y3
      complex JKRZ
      complex Ex,Ey,Ez,Extot,Eytot,Eztot,Exknt,Eyknt,Ezknt
      external Ex,Ey,Ez

      pi=acos(-1.0)
      Convert the angles from degrees into radians
      alr=ald*pi/180.
      a2r=a2d*pi/180.

```

```

a3r=a3d*pi/180.
C Now calculate the elements of the Rotation Transformation Matrix, Rij
c1=cos(a1r)
c2=cos(a2r)
c3=cos(a3r)
s1=sin(a1r)
s2=sin(a2r)
s3=sin(a3r)
R11=c3*c2*c1-s3*s2
R12=c3*s2*c1+s3*c2
R13=-c3*s1
R21=-s3*c2*c1-c3*s2
R22=-s3*s2*c1+c3*c2
R23=s3*s1
R31=s1*c3
R32=s1*s2
R33=c1

C'////////////////////////////////////]
C           Now Enter the Wavenumber ]
C   make sure that f is in MHz      ]
C   beta=(2.*pi*freq)/300.          ]
C.....]

C'////'Now Enter the data points !'////]
C ]
C   call rotate(xdtil,ydtil,zdtil,xd,yd,zd,nd,a1r,a2r,a3r) ]
C ]
C.....]

C'////////////////////////////////////]
C           Now Enter The Observation Points ]
C   read(5,*)nob ]
C   do 3 k=1,nob ]
C   read(5,*)Xob(k),Yob(k),Zob(k) ]
C   3 continue ]
C   call rotate(xotil,yotil,zotil,xob,yob,zob,nob,a1r,a2r,a3r) ]
C.....]

C'////////////////////////////////////]
C ]
C   create the (r,s) pairs. These are the points where the ]
C   value of the integrand is needed in the r-s system. In ]
C   this system the triangular domain is the square (-1,1) X (-1,1). ]
C ]
C   if(ngauss.eq.4) call gauss4(ngauss,gz,gw)
C   if(ngauss.eq.6) call gauss6(ngauss,gz,gw)
C   if(ngauss.eq.8) call gauss8(ngauss,gz,gw)

```

```

if(ngauss.eq.10) call gaus10(ngauss,gz,gw)
if(ngauss.eq.12) call gaus12(ngauss,gz,gw)
if(ngauss.eq.16) call gaus16(ngauss,gz,gw)
if(ngauss.eq.48) call gaus48(ngauss,gz,gw)

```

```

C.....]

```

```

C'.....]

```

```

C      Create the [u,v] pairs.  These are the points where the
C      value of the integrand is needed in the u-v system.  In this
C      system the domain is a right triangular defined by the points :
C      (x1,y1) <-> [0,0]      (x2,y2) <-> [1,0]      (x3,y3) <-> [0,1]

```

```

      call rstouv(ngauss,gz,u,v)

```

```

C.....]

```

```

C.....]

```

```

C'.....]

```

```

C      Now run ibiran for the first time

```

```

C      Create the point mess

```

```

      iop(1)=0

```

```

      iop(2)=0

```

```

      maxnxi=1

```

```

      nxi=1

```

```

      nyi=1

```

```

      xi=(xd(1)+xd(2)+xd(3)+xd(4))/4.

```

```

      yi=(yd(1)+yd(2)+yd(3)+yd(4))/4.

```

```

      call ibiran(nd,xd,yd,zd,iop,maxnxi,nxi,xi,nyi,yi,zi,iwk,wk,ierr)

```

```

      nt=iwk(5)

```

```

C      nl=iwk(6)

```

```

C      write(2,*)"# of triangles =",nt,"      nl =",nl

```

```

C.....]

```

```

C'.....]

```

```

C.....]

```

```

C      This is the loop for each observation point

```

```

      do 6 lobe=1,nob

```

```

      Xo=Xob(lobe)

```

```

      Yo=Yob(lobe)

```

```

      Zo=Zob(lobe)

```

```

      Extot=(0.0,0.0)

```

```

      Eytot=(0.0,0.0)

```

```

      Eztot=(0.0,0.0)

```

```

C'.....]

```

```

C      This is the LOOP that deals with each triangle

```

```

C.....]

```

```

C   The barycentric point is found of each triangle and      ]
C   the ibiran is called in order to calculate the coef-    ]
C   ficients of the polynomial in the u-v system at the     ]
C   triangle in question.                                     ]

do 5 knt=1,nt

  iop(1)=0
  iop(2)=2
  nxi=1
  nyi=1
  maxnxi=1
  kk=15+3*knt

  x1=xd(iwk(kk-2))
  y1=yd(iwk(kk-2))
  x2=xd(iwk(kk-1))
  y2=yd(iwk(kk-1))
  x3=xd(iwk(kk))
  y3=yd(iwk(kk))

  a=x2-x1
  b=x3-x1
  c=y2-y1
  d=y3-y1
  abcd= a*d - b*c

  UparX=  d / abcd
  VparX= -c / abcd

C   The coordinates of the Barycentric point of the knt-th  ]
C   triangle follow                                           ]

  xbaryc = (x1 + x2 + x3) / 3.0
  ybaryc = (y1 + y2 + y3) / 3.0

C   Run IBIRAN in order to create the coefficients of the poly- ]
C   nomial that describes the surface in the u-v system. To make ]
C   sure that the correct triangle is considered IBIRAN is asked ]
C   to run for the BARYCENTRIC POINT of the triangle. This point ]
C   lies in the triangle no matter what !!!!!!!!!!!!!!!!!!!!!!! ]

  call ibiran(nd,xd,yd,zd,iop,maxnxi,nxi,xbaryc,nyi,ybaryc,
1          zbaryc,iwk,wk,ierr)

C   Create the (x,y) pairs. These are the points where the    ]
C   value of the integrand is needed in the x-y system. In    ]

```

```

C      this system the triangular domain is defined by the points ]
C      (x1,y1),      (x2,y2)      and      (x3,y3) ]
C      ]
C      call uvtoxy(ngauss,x,y,u,v,x1,x2,x3,y1,y2,y3) ]
C      ]
C      Create the Z and Zx values.  Z(k,j) is the value of ]
C      the reflector surface Z=Z(x,y) calculated at the point ]
C      x=x(k,j) , y=y(k,j) .  Zx(k,j) is the value of the partial ]
C      derivative of Z with respect to x at the aforementioned ]
C      point      - (x(k,j), y(k,j)) - ]

```

```

do 50 k=1,ngauss
uk=u(k)
do 49 j=1,ngauss
vkj=v(k,j)
as0=P00+ vkj*(P01+ vkj*(P02+ vkj*(P03+ vkj*(P04+ vkj*P05))))
as1=P10+ vkj*(P11+ vkj*(P12+ vkj*(P13+ vkj*P14)))
as2=P20+ vkj*(P21+ vkj*(P22+ vkj*P23))
as3=P30+ vkj*(P31+ vkj*P32)
as4=P40+ vkj*P41
Z(k,j)=as0+ uk*(as1+ uk*(as2+ uk*(as3+ uk*(as4+ uk*P50))))
Zu=as1+ uk*(2.*as2+ uk*(3.*as3+ uk*(4.*as4+ uk*5.*P50)))
as0=P01+ vkj*(2.*P02+ vkj*(3.*P03+ vkj*(4.*P04+ vkj*5.*P05)))
as1=P11+ vkj*(2.*P12+ vkj*(3.*P13+ vkj*4.*P14))
as2=P21+ vkj*(2.*P22+ vkj*3.*P23)
as3=P31+ vkj*2.*P32
Zv=as0+ uk*(as1+ uk*(as2+ uk*(as3+ uk*P41 )))
Zx(k,j)= Zu*UparX + Zv*Vparx
49 continue
50 continue

```

```

C      Create the array Ro(k,j).  This array contains the distance
C      of the point ( x(k,j),y(k,j),z(k,j) ) from the observation
C      point ( Xo,Yo,Zo ) .
C      ALSO
C      Create the complex arrays SCA(k,j).  These arrays contain ]
C      the common coefficients in front of all the field compo- ]
C      nents. ]

```

```

do 58 k=1,ngauss
do 57 j=1,ngauss
Ro(k,j)=sqrt( (x(k,j)-Xo)*(x(k,j)-Xo) +
1          (y(k,j)-Yo)*(y(k,j)-Yo) +
2          (z(k,j)-Zo)*(z(k,j)-Zo) )
RR=Ro(k,j)
JKRZ=cmlpx( 0.0, -beta * (RR-z(k,j)) )
SCA1(k,j)= cexp(JKRZ) / RR
SCA2(k,j)= cmlpx(beta*beta - 3.0/(RR*RR), -3.0*beta/RR) *
1          ( Xo-x(k,j) + (Zo-z(k,j))*Zx(k,j) )/RR
SCA3(k,j)= cmlpx( 1.0/(RR*RR)-beta*beta , beta/RR )

```

C.....72

57 continue
58 continue

```

C*****
C    Call the "CALINT" subroutine to calculate the          *
C    Integrals on each triangular domain                    *

      call calint(Ex,ngauss,x,y,z,zx,Ro,SCA1,SCA2,SCA3,Exknt,gw,gz,u,v)
      call calint(Ey,ngauss,x,y,z,zx,Ro,SCA1,SCA2,SCA3,Eyknt,gw,gz,u,v)
      call calint(Ez,ngauss,x,y,z,zx,Ro,SCA1,SCA2,SCA3,Ezknt,gw,gz,u,v)

C*****
C*****
      Extot=Extot + Exknt
      Eytot=Eytot + Eyknt
      Eztot=Eztot + Ezknt
5  continue
      Extot=Extot/cmplx(1.0 , 2.0*pi*beta)
      Eytot=Eytot/cmplx(1.0 , 2.0*pi*beta)
      Eztot=Eztot/cmplx(1.0 , 2.0*pi*beta)

C'''' Transform the E-fields back to the tilded coordinate system '''' ]
C
      Estil(1,lobe)=R11*Extot+R21*Eytot+R31*Eztot
      Estil(2,lobe)=R12*Extot+R22*Eytot+R32*Eztot
      Estil(3,lobe)=R13*Extot+R23*Eytot+R33*Eztot
C.....72
C    write(3,*)" ",R11*Xo+R21*Yo+R31*Zo,"correct"
C    write(3,*)" ",R12*Xo+R22*Yo+R32*Zo,"correct"
C    write(3,*)" ",R13*Xo+R23*Yo+R33*Zo,"correct"
C    write(3,*)" ",Xotil(lobe),Yotil(lobe),Zotil(lobe),"coord. in til"
C    write(3,*)" ",Estil(1,lobe)," Esxtil"
C    write(3,*)" ",Estil(2,lobe)," Esytil"
C    write(3,*)" ",Estil(3,lobe)," Esztil"
C    write(3,*)" "
C.....]

      6 continue

      return
      end

C.....72

C    This subroutine rotates the antenna as well as the observation
C    points into the incident wave coordinate system !

```

C

```
subroutine rotate(Axt,Ayt,Azt,Ax,Ay,Az,n,a1,a2,a3)
dimension Ax(n),Ay(n),Az(n),Axt(n),Ayt(n),Azt(n)
```

```
c1=cos(a1)
c2=cos(a2)
c3=cos(a3)
s1=sin(a1)
s2=sin(a2)
s3=sin(a3)
R11=c3*c2*c1-s3*s2
R12=c3*s2*c1+s3*c2
R13=-c3*s1
R21=-s3*c2*c1-c3*s2
R22=-s3*s2*c1+c3*c2
R23=s3*s1
R31=s1*c3
R32=s1*s2
R33=c1
```

```
do 1 i=1,n
Ax(i)= R11*Axt(i) + R12*Ayt(i) + R13*Azt(i)
Ay(i)= R21*Axt(i) + R22*Ayt(i) + R23*Azt(i)
Az(i)= R31*Axt(i) + R32*Ayt(i) + R33*Azt(i)
1 continue
```

```
return
end
```

C.....72

```
subroutine calint(f,n,x,y,z,zx,Ro,SCA1,SCA2,SCA3,result,gw,gz,u,v)
dimension u(n),v(n,n),x(n,n),y(n,n),z(n,n),zx(n,n)
real Ro(n,n)
complex SCA1(n,n),SCA2(n,n),SCA3(n,n)
dimension gw(n),gz(n)
double precision gw,gz
COMMON /IBCDPT/ X0,Y0,AP,BP,CP,DP,P00,P10,P20,P30,P40,P50,
1 P01,P11,P21,P31,P41,P02,P12,P22,P32,P03,P13,
2 P23,P04,P14,P05,ITPV
common /vertex/ x1,x2,x3,y1,y2,y3
complex f,Tkj,result,res
external f
```

C

C

C

C

C

C

C

C

C

This program calculates the double integral

$$I = \int \int f(x,y,z,zx) \, dx \, dy \quad \text{on a triangular domain}$$

where $z=z(x,y)$ and zx is $\partial z / \partial x$ (also function of x,y).
The domain is determined by the vertices of the triangle
 (x_1,y_1) , (x_2,y_2) and (x_3,y_3) GIVEN COUNTERCLOCKWISE !!!
If the vertices are not arranged counterclockwise then

the value of I is the opposite of what it should be !!!!

abcd as calculated below is the Jacobian of the mapping from the x-y to the u-v system. It is equal to the ratio of the areas of the triangular domain in the two systems. Since in the u-v system the triangle is always given by the points [0,0], [1,0] and [0,1], in this system its area is $1/2$. Thus, it is not a surprise that abcd equals twice the area of the triangle in the x-y system (defined by the points (x1,y1), (x2,y2) and (x3,y3)) !!!!!!!!!!!!!!!!!!!!!!!

```

a=x2-x1
b=x3-x1
c=y2-y1
d=y3-y1
abcd= a*d - b*c
if(abcd.eq.0.0) goto 666

```

Calculate the integral by using Gaussian Quadrature in 2-dimensions. For the algorithm see my notes.

This part of the subroutine calculates the values of the function $T(r,s)$ at the points that are used by the Gauss-Legendre quadrature method. These values are used in the main in a summation scheme to provide the approximation to the integral. Since in this program we have used $m=n$, $r(k)$ and $s(k)$ are exactly the same. For a more general approach read my notes.

A very important note should be made here. abcd is the value of the Jacobian of the mapping from the x-y to u-v. Since abcd is not the absolute value of the Jacobian one needs to make sure that the points (x1,y1), (x2,y2) & (x3,y3) are ordered counterclockwise. For more details look up my notes.

```

result=(0.0,0.0)
res=(0.0,0.0)
do 2 k=1,n
  do 1 j=1,n
    Tkj=0.125 * (1.-gz(k)) * abcd *
1      f( x(k,j),y(k,j),z(k,j),zx(k,j),Ro(k,j),
2        SCA1(k,j),SCA2(k,j),SCA3(k,j) )
    res=res + gw(j) * Tkj
1  continue
  result=result + gw(k) * res
  res=(0.0,0.0)
2  continue
  go to 667
666 write(0,*)"There is something wrong with the triangle.",
1"Colinear vertices."
667 continue

```

```

return
end

```

```

subroutine uvtoxy(n,x,y,u,v,x1,x2,x3,y1,y2,y3)
dimension u(n),v(n,n),x(n,n),y(n,n)

```

```

a=x2-x1
b=x3-x1
c=y2-y1
d=y3-y1
abcd= a*d - b*c

```

```

do 2 k=1,n
do 1 j=1,n
x(k,j)=x1 + a * u(k) + b * v(k,j)
y(k,j)=y1 + c * u(k) + d * v(k,j)
1 continue
2 continue

```

```

return
end

```

```

subroutine rstouv(n,gz,u,v)
dimension gz(n),u(n),v(n,n)
double precision gz

```

```

do 1 k=1,n
u(k)=0.5 + 0.5*gz(k)
1 continue

do 3 k=1,n
do 2 j=1,n
v(k,j)=(1.0-gz(k)) * (1.0+gz(j)) / 4.0
2 continue
3 continue

```

```

return
end

```

```

C      complex function Ex(x,y,z,zx,Ro,SCA1,SCA2,SCA3)
C      Here Ro and the SCA's are constants since Ex is called by      ]
C      x(k,j),y(k,j),z(k,j),zx(k,j),Ro(k,j),SCA's(k,j)                ]
      common /observ/ Xo,Yo,Zo,beta
      complex SCA1,SCA2,SCA3

```

```

Ex=SCA1 * ( SCA2*(Xo-x)/Ro + SCA3 )
return
end

```

```

C      complex function Ey(x,y,z,zx,Ro,SCA1,SCA2,SCA3)
C      Here Ro and the SCA's are constants since Ey is called by      ]
C      x(k,j),y(k,j),z(k,j),zx(k,j),Ro(k,j),SCA's(k,j)                ]
      common /observ/ Xo,Yo,Zo,beta
      complex SCA1,SCA2,SCA3

```

```

Ey=SCA1 * SCA2*(Yo-y)/Ro
return
end

```

```

C      complex function Ez(x,y,z,zx,Ro,SCA1,SCA2,SCA3)
C      Here Ro and the SCA's are constants since Ez is called by      ]
C      x(k,j),y(k,j),z(k,j),zx(k,j),Ro(k,j),SCA's(k,j)                ]
      common /observ/ Xo,Yo,Zo,beta
      complex SCA1,SCA2,SCA3

```

```

Ez=SCA1 * ( SCA2*(Zo-z)/Ro + SCA3*zx )
return
end

```

```

C      subroutine gauss4(n,z,w)
      double precision z,w
      dimension z(n),w(n)
      n=4
      nn=n/2

```

```

      z(1)=.339981043584856d0
      z(2)=.861136311594053d0

```

```

      w(1)=.652145154862546d0
      w(2)=.347854845137454d0

```

```

      do 1 k=1,nn
        z(nn+k)=-z(k)
        w(nn+k)=w(k)
1      continue

```

```

      do 2 k=1,nn
        z(k)=-z(n+1-k)
        w(k)=w(n+1-k)
2      continue
      return
end

```

C

C

```

subroutine gauss6(n,z,w)
double precision z,w
dimension z(n),w(n)
n=6
nn=n/2

```

```

z(1)=.238619186083197d0
z(2)=.661209386466265d0
z(3)=.932469514203152d0

```

```

w(1)=.467913934572691d0
w(2)=.360761573048139d0
w(3)=.171324492379170d0

```

```

do 1 k=1,nn
z(nn+k)=-z(k)
w(nn+k)=w(k)
1 continue

```

```

do 2 k=1,nn
z(k)=-z(n+1-k)
w(k)=w(n+1-k)
2 continue
return
end

```

C
C

```

subroutine gauss8(n,z,w)
double precision z,w
dimension z(8),w(8)

```

C
C
C
C
C
C
C
C
C
C
C

The array z contains the zeros of the Legendre polynomial of the 8th degree. The array w contains the appropriate weights for the Gaussian quadrature. The values of w(k) are given by

$$w(i) = 2 / ((1 - z(i)**2) * (P'(z(i))**2))$$

where $P(z(i)) = 0$ $i = 1, 2, \dots, 8$
and $P'(z) = dP(z)/dz$

```

n=8
nn=n/2

```

```

z(1)=.183434642495650d0
z(2)=.525532409916329d0
z(3)=.796666477413627d0
z(4)=.960289856497536d0

```

```

w(1)=.362683783378362d0
w(2)=.313706645877887d0
w(3)=.222381034453374d0
w(4)=.101228536290376d0

```

```

do 1 k=1,nn
z(nn+k)=-z(k)
w(nn+k)=w(k)
1 continue

```

```

do 2 k=1,nn
z(k)=-z(n+1-k)
w(k)=w(n+1-k)
2 continue
return
end

```

c
c

```

subroutine gaus10(n,z,w)
double precision z,w
dimension z(n),w(n)

```

```

n=10
nn=n/2

```

```

z(1)=.148874338981631d0
z(2)=.433395394129247d0
z(3)=.679409568299024d0
z(4)=.865063366688985d0
z(5)=.973906528517172d0

```

```

w(1)=.295524224714753d0
w(2)=.269266719309996d0
w(3)=.219086362515982d0
w(4)=.149451349150581d0
w(5)=.066671344308688d0

```

```

do 1 k=1,nn
z(nn+k)=-z(k)
w(nn+k)=w(k)
1 continue

```

```

do 2 k=1,nn
z(k)=-z(n+1-k)
w(k)=w(n+1-k)
2 continue
return
end

```

C
C

```

subroutine gaus12(n,z,w)
double precision z,w
dimension z(n),w(n)
n=12
nn=n/2

```

```

z(1)=.125233408511469d0
z(2)=.367831498998180d0
z(3)=.587317954286617d0
z(4)=.769902674194305d0
z(5)=.904117256370475d0
z(6)=.981560634246719d0

```

```

w(1)=.249147045813403d0
w(2)=.233492536538355d0
w(3)=.203167426723066d0
w(4)=.160078328543346d0
w(5)=.106939325995318d0
w(6)=.047175336386512d0

```

```

do 1 k=1,nn
z(nn+k)=-z(k)
w(nn+k)=w(k)
1 continue

```

```

do 2 k=1,nn
z(k)=-z(n+1-k)
w(k)=w(n+1-k)
2 continue
return
end

```

C
C

```

subroutine gaus16(n,z,w)
double precision z,w
dimension z(8),w(8)

```

C
C
C
C
C
C
C
C
C
C
C

The array z contains the zeros of the Legendre polynomial of the 16th degree. The array w contains the appropriate weights for the Gaussian quadrature. The values of w(k) are given by

$$w(i) = 2 / ((1 - z(i)**2) * (P'(z(i))**2))$$

where $P(z(i)) = 0$ $i = 1, 2, \dots, 16$
and $P'(z) = dP(z)/dz$

```

n=16

```

```
nn=n/2
```

```
z(1)=.095012509836637440185d0
z(2)=.281603550779258913230d0
z(3)=.458016777657227386342d0
z(4)=.617876244402643748447d0
z(5)=.755404408355003033895d0
z(6)=.865631202387831743880d0
z(7)=.944575023073232576078d0
z(8)=.989400934991649932596d0
```

```
w(1)=.189450610455068496285d0
w(2)=.182603415044923558867d0
w(3)=.169156519395002538189d0
w(4)=.149595988816576732081d0
w(5)=.124628971255533872052d0
w(6)=.095158511682492784810d0
w(7)=.062253523938647892863d0
w(8)=.027152459411754094852d0
```

```
do 1 k=1,nn
  z(nn+k)=-z(k)
  w(nn+k)=w(k)
1 continue
```

```
do 2 k=1,nn
  z(k)=-z(n+1-k)
  w(k)=w(n+1-k)
2 continue
```

```
return
end
```

```
subroutine gaus48(n,z,w)
```

The array z contains the zeros of the Legendre polynomial of the 48th degree. The array w contains the appropriate weights for the Gaussian quadrature. The values of w(k) are given by

$$w(i) = 2 / ((1-z(i)**2) * (P'(z(i))**2))$$

where $P(z(i))=0$ $i=1,2,\dots,48$
and $P'(z)=dP(z)/dz$

```
dimension z(n),w(n)
double precision z,w
```

n=48
nn=n/2

z(1) =.032380170962869362033d0
z(2) =.097004699209462698930d0
z(3) =.161222356068891718056d0
z(4) =.224763790394689061225d0
z(5) =.287362487355455576736d0
z(6) =.348755886292160738160d0
z(7) =.408686481990716729916d0
z(8) =.466902904750958404545d0
z(9) =.523160974722233033678d0
z(10) =.577224726083972703818d0
z(11) =.628687396776513623995d0
z(12) =.677872379632663905212d0
z(13) =.724034130923814654674d0
z(14) =.767159032515740339254d0
z(15) =.807066204029442627083d0
z(16) =.843588261624393530711d0
z(17) =.876572020274247885906d0
z(18) =.905879136715569672822d0
z(19) =.931386690706554333114d0
z(20) =.952987703160430860723d0
z(21) =.970591592546247250461d0
z(22) =.984124583722826857745d0
z(23) =.993530172266350757548d0
z(24) =.998771007252426118601d0

w(1) =.064737696812683922503d0
w(2) =.064466164435950082207d0
w(3) =.063924238584648186624d0
w(4) =.063114192286254025657d0
w(5) =.062039423159892663904d0
w(6) =.060704439165893880053d0
w(7) =.059114839698395635746d0
w(8) =.057277292100403215705d0
w(9) =.055199503699984162868d0
w(10) =.052890189485193667096d0
w(11) =.050359035553854474958d0
w(12) =.047616658492490474826d0
w(13) =.044674560856694280419d0
w(14) =.041545082943464749214d0
w(15) =.038241351065830706317d0
w(16) =.034777222564770438893d0
w(17) =.031167227832798088902d0
w(18) =.027426509708356948200d0
w(19) =.023570760839324379141d0
w(20) =.019616160457355527814d0
w(21) =.015579315722943848728d0
w(22) =.011477234579234539490d0
w(23) =.007327553901276262102d0
w(24) =.003153346052305838633d0

```
do 1 k=1,nn  
  z(nn+k)=-z(k)  
  w(nn+k)=w(k)  
1 continue
```

```
do 2 k=1,nn  
  z(k)=-z(n+1-k)  
  w(k)=w(n+1-k)  
2 continue  
  return  
end
```

c